STUDY ON HEAD OVERCOAT THICKNESS OF HEAD GIMBAL ASSEMBLY FOR HEAD MEDIA SPACING REDUCTION

SARINYA KHAMDEE

A THESIS SUBMITTED IN PARTIAL FULFILLMENT
OF THE REQUIREMENT FOR THE DEGREE OF
MASTER OF ENGINEERING IN DATA STORAGE TECHNOLOGY
INTERNATIONAL COLLEGE
KING MONGKUT'S INSTITUTE OF TECHNOLOGY LADKRABANG
2014

KMITL-2014-IC-M-005-009

STUDY ON HEAD OVERCOAT THICKNESS OF HEAD GIMBAL ASSEMBLY FOR HEAD MEDIA SPACING REDUCTION

SARINYA KHAMDEE

A THESIS SUBMITTED IN PARTIAL FULFILLMENT

OF THE REQUIREMENT FOR THE DEGREE OF

MASTER OF ENGINEERING IN DATA STORAGE TECHNOLOGY

INTERNATIONAL COLLEGE

KING MONGKUT'S INSTITUTE OF TECHNOLOGY LADKRABANG

2014

KMITL-2014-IC-M-005-009

หัวข้อวิทยานิพนธ์	การศึกษาความหนาของชั้นเคลือบหัวอ่านของชุดประกอบหัวอ่านและเขียนสำหรับการลดระยะห่างระหว่างหัวอ่านแและแผ่นบันทึกข้อมูล
นักศึกษา	นางสาวศรินยา คำดี
รหัสประจำตัว	53600618
ปริญญา	วิศวกรรมศาสตรมหาบัณฑิต
สาขาวิชา	เทคโนโลยีการบันทึกข้อมูล
พ.ศ.	2557
อาจารย์ที่ปรึกษาวิทยานิพนธ์	ผู้ช่วยศาสตราจารย์ ดร.วินัดดา วงศ์วิริยะพันธ์

บทคัดย่อ

ในงานวิจัยนี้ได้ศึกษาความหนาของชั้นเคลือบหัวอ่าน (Head overcoat, HOC) ของชุดประกอบหัวอ่านและเขียน (Head gimbal assembly, HGA) สำหรับการลดระยะห่างระหว่างหัวอ่านแและแผ่นบันทึกข้อมูล (Head media spacing, HMS) ในการศึกษาได้เตรียมหัวอ่านที่เคลือบด้วย HOC ที่ความหนาแตกต่างกัน โดย HOC ประกอบไปด้วยชั้นคาร์บอนและชั้นสารยึดติดสำหรับยึดติดชั้นคาร์บอนและแผ่นบันทึกข้อมูล ความหนาของ HOC ที่ใช้ในงานวิจัยมี 3 ชนิด ได้แก่ HOC 16, 20 และ24 อังสตรอม โดย HOC 16 อังสตรอม ประกอบด้วยชั้นสารยึดติดชนิด A (Adhesion layer) และชั้นคาร์บอนชนิด C HOC 20 อังสตรอม ประกอบด้วยชั้นสารยึดติดชนิด B (Adhesion layer) และชั้นคาร์บอนชนิด C และ HOC 24 อังสตรอม ประกอบด้วยชั้นสารยึดติดชนิด B (Adhesion layer) และชั้นคาร์บอนชนิด D โดยชั้นสารยึดติดชนิด A มีความหนาที่บางกว่าชั้นสารยึดชนิด B และชั้นคาร์บอนชนิด C มีความหนาที่บางกว่าชั้นคาร์บอนชนิด D HOC ทั้ง 3 ชนิด ถูกนำมาทดสอบสมบัติความน่าเชื่อถือในด้านการกัดกร่อน ประสิทธิภาพในการอ่านเขียน และการเกิดการสึกหรอ สำหรับการทดสอบการกัดกร่อน ได้ทำการทดลองบนเครื่องจักรสำหรับการจำลองสภาวะที่เร่งเกิดการกัดกร่อนขั้นสูง (High accelerate stress test, HAST) พบว่า HOC ทุกความหนานั้น มีจำนวนตำแหน่งที่เกิดการกัดกร่อนอยู่ในขอบเขตที่ยอมรับได้ สำหรับการทดสอบประสิทธิภาพในการอ่านเขียน ได้ทำการทดสอบโดยใช้เครื่องจักรสำหรับการวัดค่าทางไฟฟ้าของชุดประกอบหัวอ่าน โดยการถูหัวอ่าน (Burnishing) ที่ตำแหน่ง +1 นาโนเมตร จนถึง -4 นาโนเมตร โดยค่าทางไฟฟ้าที่ทำการศึกษาได้แก่ ค่ากำลังไฟฟ้าสำหรับให้หัวอ่านสัมผัสกับแผ่นบันทึกข้อมูล ค่าเคลียแรนซ์ ค่าอัตราความผิดพลาดบิต ค่าโอเวอร์ไรท์ ค่าแอมพลิจูด และค่าความต้านทานของส่วนอ่าน พบว่า HOC 16 อังสตรอม มีค่าการเปลี่ยนแปลงของค่าทางไฟฟ้าต่างๆก่อนและหลังการถูหัวอ่านน้อยที่สุด โดย ณ ตำแหน่ง –4 นาโนเมตร มีการเปลี่ยนแปลงของค่าอัตราความผิดพลาดบิต ค่าโ

อเวอร์ไรท์ ค่าแอมพลิจูด และค่าความต้านทานของส่วนอ่าน เป็น 0.22 เดคเคด 2.70 เดซิเบล 3.84 เปอร์เซนต์ และ 2.38 เปอร์เซนต์ ตามลำดับ แสดงถึงประสิทธิภาพในการอ่านและเขียนที่ค่อนข้างคงที่ สำหรับการทดสอบการสึกหรอ ได้นำหัวอ่านที่ผ่านการถูหัวอ่าน มาวิเคราะห์ด้วยกล้องจุลทรรศน์แรงอะตอมและกล้องจุลทรรศน์อิเลกตรอยแบบส่องกราด พบว่า HOC 16 อังสตรอม เกิดรอยลึกของส่วนอ่านและส่วนเขียนที่ตื้นที่สุด โดยมีความลึก 1.6 และ 1.7 นาโนเมตร ตามลำดับ นอกจากนี้ HOC 16 อังสตรอม ยังมีพื้นที่ที่เกิดการสึกหรอน้อยที่สุด โดยพื้นที่ที่การสึกหรอในส่วนอ่านและส่วนเขียนเป็น 21 และ 54 ตารางไมโครเมตรตามลำดับ จากผลการทดสอบพบว่า ความหนาของชั้นเคลือบหัวอ่าน 16 อังสตรอม เป็นเงื่อนไขที่ดีที่สุดสำหรับลดระยะระหว่างหัวอ่านและแผ่นบันทึกข้อมูล โดยชั้นสารยึดติดซึ่งมีความหนาที่บางและสามารถสร้างพันธะที่ดีกับชั้นคาร์บอนเป็นปัจจัยที่ทำให้หัวอ่านยังคงสมบัติความน่าเชื่อถือที่ดีไว้ได้

Thesis Title: Study on Head Overcoat Thickness of Head Gimbal Assembly for Head Media Spacing Reduction
Student: Miss Sarinya Khamdee
Student ID: 53600618
Degree: Master of Engineering
Program: Data Storage Technology
Year: 2014
Thesis Advisor: Assistant Professor Dr. Winadda Wongwiriyapan

ABSTRACT

In this study, effect of head overcoat (HOC) thickness of head gimbal assembly (HGA) for head media spacing (HMS) reduction was investigated. HOC consists of diamond-like carbon (DLC) layer and adhesion layer for bonding DLC and magnetic layer. Three types of HOC thickness were used in this study; HOC 16, 20 and 24 Å. HOC 16 Å consists of adhesion layer type A and DLC layer type C. HOC 20 Å consists of adhesion layer type B and DLC layer type C. HOC 24 Å consist of adhesion layer type B and DLC layer type D. Thickness of adhesion layer type A is thinner than that of type B and thickness of DLC layer type C is thinner than that of type D. Each HOC was characterized its reliability properties in terms of corrosion, read/write performance and wear. For corrosion characterization, each HOC was treated by high accelerate stress test (HAST). After HAST, all HOCs show a number of corrosion position in acceptable range. For read/write performance characterization, each HOC was treated on spin-stand tester for electrical measurement of HGA by burnishing at interference level from +1 to -4 nm. Each HOC was characterized its electrical properties in terms of power to contact (PtC), clearance, bit error rate (BER), overwrite (OVW), amplitude (AMP) and reader resistance (RD_RES) before and after burnishing. HOC 16 Å showed the least delta value of each electrical property at interference level of -4 nm. Its delta BER, OVW, AMP and RD_RES are 0.22 decade, 2.70 dB, 3.84% and 2.38%, respectively. These results imply a stable read/write performance of HOC 16 Å. For wear characterization, HGA after burnishing process was characterized by atomic force microscopy (AFM) and field emission scanning

electron microscopy (FESEM). HOC 16 Å showed the shallowest wear depth of writer and reader as 1.6 and 1.7 nm, respectively. Moreover, HOC 16 Å shows the smallest wear area of writer and reader as 21 and 54 μm^2, respectively. From all reliability test results, HOC 16 Å is the optimum condition for head media spacing reduction. Thin adhesion layer and a good bonding between DLC and magnetic layer is a key for a good reliability.

ACKNOWLEDGEMENTS

This thesis could not be completed without assistance from many persons whom I would like to express my sincere appreciation.

First of all, I would like to sincerely thankful my advisor Assistance Professor Dr.Winadda Wongwiriyapan, who always gives helpful suggestions, useful advice, quickly response and be patient to work with me during my research work.

Secondly, I am really grateful to Seagate Technology (Thailand), the National Science and Technology Development Agency (NSTDA) and King Mongkut's Institute of Technology Ladkrabang (KMITL), who gives nicely opportunity and provides the full scholarship to study the master program.

Finally, I am really thankful to my family for everything throughout my life, my managers and colleagues especially Mr. Chanipat Euvananon and Miss Areerat Jasungnoen for their discussions on my thesis and their encouragements and my gym friends who cheer me up all the time.

Sarinya
Khamdee

CONTENTS

CONTENTS (CONT.)

LISTS OF TABLES

Tables **Page**

LISTS OF FIGURES

Figures **Page**

LISTS OF FIGURES (CONT.)

Figures **Page**

LISTS OF FIGURES (CONT.)

Figures **Page**

CHAPTER 1

INTRODUCTION

1.1 Significance and Background

Currently, due to a need to increase areal density of hard disk drive (HDD), many technologies have been developed. The main development is focused on transducer design. However, transducer design for perpendicular magnetic recording (PMR) is nearly to reach its limitation, and technology will be switched to heat assist magnetic recording (HAMR) in the near future. **Figure1.1** shows areal density trend. Prior to changing to HAMR technology, the critical approach to reach higher areal density for PMR technology is head media spacing (HMS) reduction. HMS is head overcoat including touch down height, clearance, media lubricant and media overcoat [1].There are many technologies have been developed to reduce HMS such as air bearing design, thermo mechanical design, media overcoat and head overcoat (HOC).

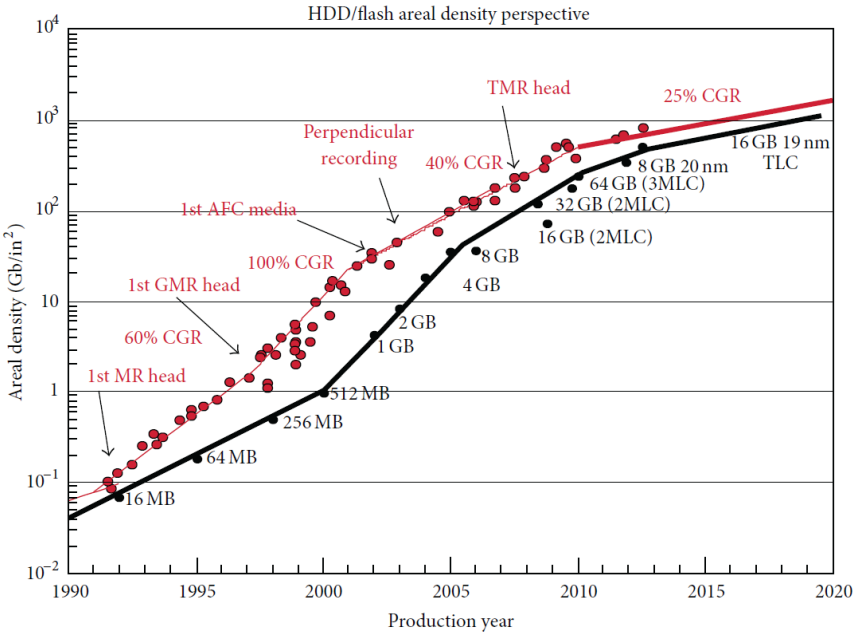

Figure 1.1 Areal density trend [1].

Currently, HMS is ca. 12-15 nm and fly height is ca. 10 nm. To increase areal density, it is estimated that the HMS should be lower than 10 nm. There were many studied on HMS reduction such as media overcoat reduction.

To reach a goal of areal density of 1 Tb/in^2 or higher, overcoat is required to be less than 2 nm. Y. Nobuto *et al.* studied on head overcoat reduction. Diamond like carbon (DLC) forming technique, thickness, and substrate materials were focused, and corrosion and wear resistance of DLC on head were investigated [2]. It was found that the performance of DLC films with a few nanometers thick largely depended on their interface and substrate. SP^3 fraction, a key parameter of DLC films, can be improved by modifying substrate materials, which will improve the performance of overcoat in terms of both corrosion and wear.

Another example is media overcoat studied by K. Phetdee *et al* [3]. Wear resistance and life time of media overcoat were studied. Various adhesion layers with 15 nm DLC were used for study. Wear resistance of media overcoat was investigated by triboindentor. Life time measurement was evaluated by flying height tester. It was found that wear resistance and wear depth improved for 15 nm of DLC thickness as compare to uncoated media. Adhesion layer thickness increment is not significant for wear resistance but wear depth decrease with increment of adhesion layer. Life time has been drastically improved more than 30 times as compare to an uncoated media.

At present, media over coat still have been continuously researched to achieve the thinnest thickness with good reliability. The thickness of media over coat might be reach limitation in the near future. Thus, HOC is another factor to achieve minimum HMS and increase areal density

Although HOC is another factor to achieve minimum HMS, however, extremely thin HOC might lead to poor long term reliability. Thus, it is necessary to study the optimum thickness of HOC which maintains it is good reliability.

Previously, HOC consisted of only DLC layer, but now, HOC is DLC layer included adhesion layer. The function of adhesion layer which laid between DLC and head is to provide good bonding surface for carbon in DLC layer. The function of DLC layer is to protect head from wear and corrosion. Thus, bi-layers (DLC and adhesion layers) of HOC provide more improvement for HMS reduction such as good bonding between DLC and adhesion layer. Typically, a thickness range of HOC is ca. 20-30 Å,

which included DLC layer with a thickness of ca. 15-25 Å and adhesion layer with a thickness of ca. 5-8 Å.

In this study, taking a decrease in HOC thickness as a strategy for HMS reduction, the effect of HOC thickness on HDD performance was investigated. The reliability in terms of corrosion, read/write ability, topography and wear resistance was characterized.

1.2 Objectives

To study effect of head overcoat thickness and adhesion layer type on HGA reliability. Reliability was evaluated in terms of corrosion behavior by high accelerate stress test (HAST), read/write ability by stress burnishing on spin-stand tester, topography by atomic force microscopy and wear resistance by field emission scanning electron microscopy.

1.3 Scopes

1.3.1 Investigate corrosion behavior on transducer of various HOC thicknesses.
1.3.2 Investigate read/write ability of various HOC thicknesses.
1.3.4 Investigate wear of HOC after read/write process.
1.3.4 Investigate morphology of HOC after read/write process.

1.4 Expected Benefits

1.4.1 Obtain information of corrosion of HOC.
1.4.2 Understand read/write ability of various head overcoat thicknesses.
1.4.3 Obtain the optimum HOC thickness for the desired fly height.
1.4.4 Obtain information of wear resistance and morphology of HOC after read/write process.
1.4.5 Understand adhesion layer ability.

CHAPTER 2

THEORY AND LITERATURE REVIEWS

2.1 Head Gimbal Assemble (HGA)

In hard disk drive, there are many components included which head-gimbal assembly (HGA) is one component of hard disk drive. HGA consist of slider, flexure, load-beam, hinge and baseplate. A schematic of HGA and completed HGA is shown in **Figures 2.1 and 2.2**, respectively. Numbers 11, 12, 13, 14, 15 and 16 are magnetic head, slider, flexure, hinge, load-beam and baseplate, respectively.

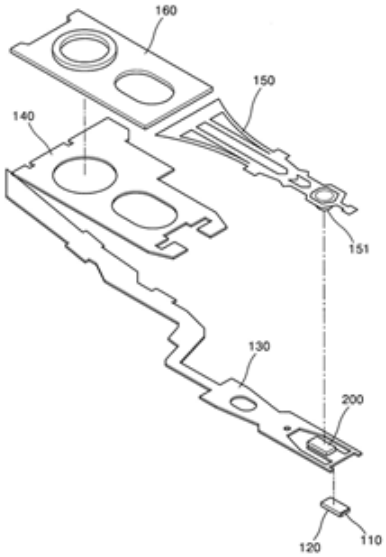

Figure 2.1 Schematic of head gimbal assembly (HGA) [5].

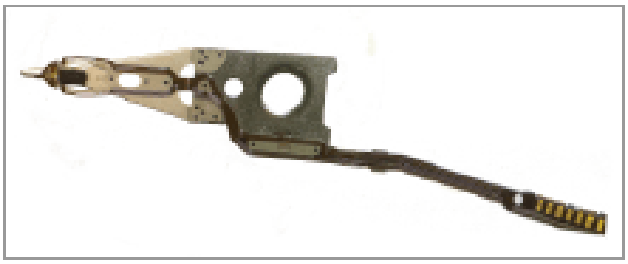

Figure 2.2 Schematic of completed HGA [www.global.tdk.com].

2.2 Head Media Spacing (HMS)

Definition of HMS is spacing between top of slider magnetic layer and media magnetic layer as shown in equation (2.1).

HMS = Media overcoat + Media lubricant + Fly height + Head overcoat (2.1)

The schematic of HMS is shown in **Figure 2.3.**

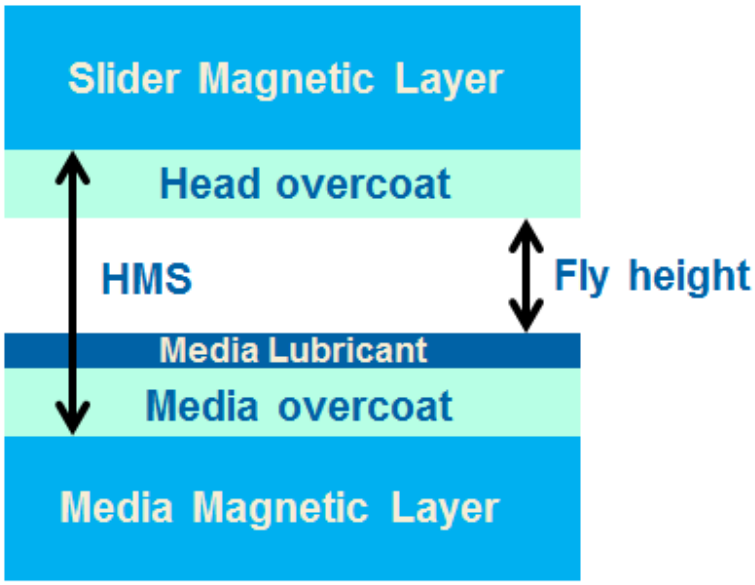

Figure 2.3 Schematic of head media spacing (HMS).

2.3 Head Overcoat (HOC)

Head overcoat is diamond-like carbon (DLC) layer including adhesion layer. A schematic of HOC layer is shown in **Figure 2.4.**

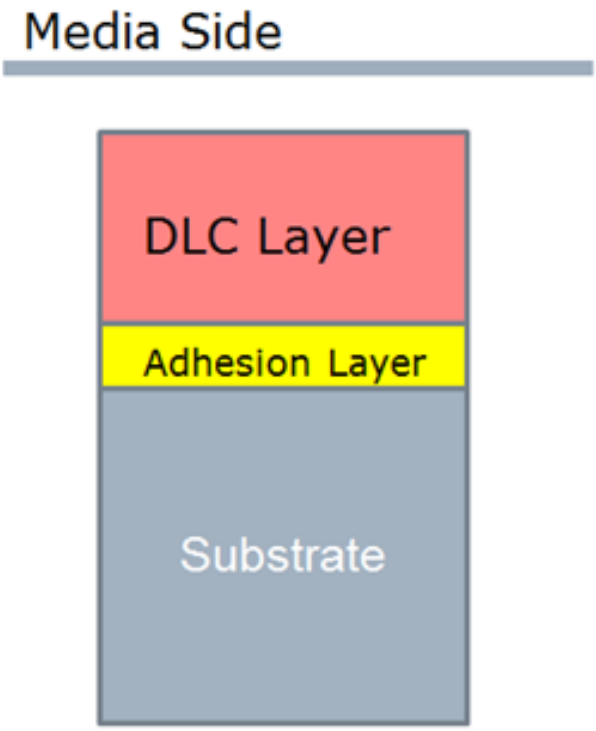

Figure 2.4 Schematic of head overcoat (HOC).

Diamond-like carbon (DLC) layer is metastable form of amorphous carbon with significant sp^3 bonding as function of DLC is used for being protective layers such as corrosion and wear for transducer because it's high mechanical hardness, chemical inertness, continuous and optical transparency.

Normally, DLC is not unique material so it is able to have any mixture of sp^3 and sp^2 site with possible presence hydrogen and nitrogen. The composition of nitrogen-free carbon films are conveniently as shown in **Figure 2.5.**

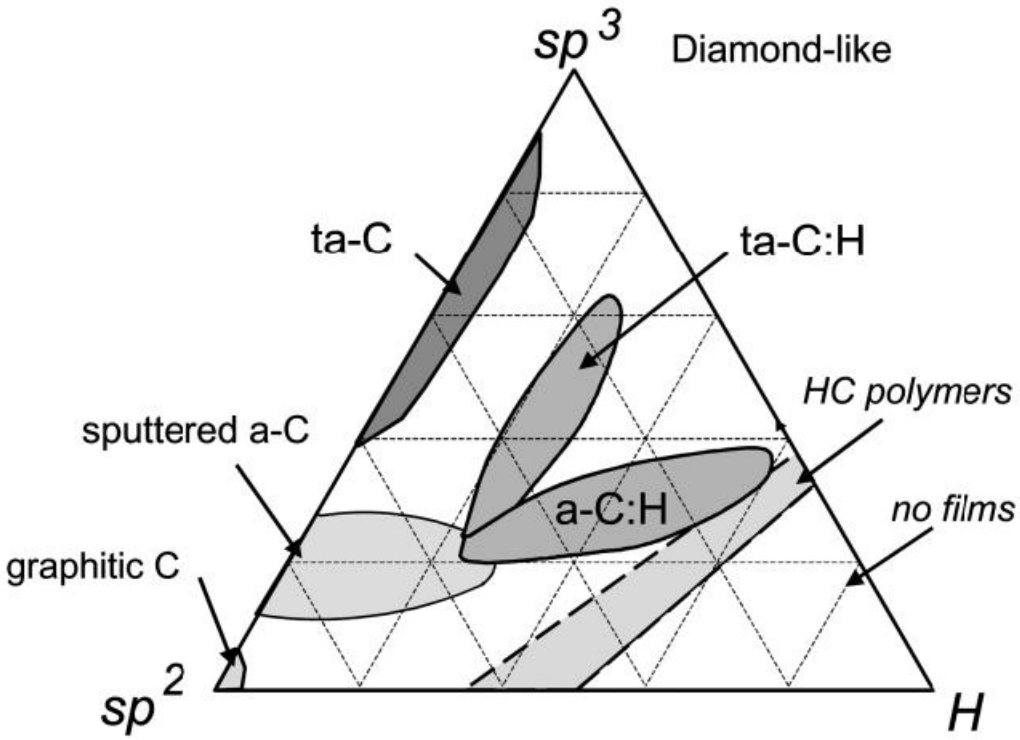

Figure 2.5 Ternary phase diagram of amorphous carbons [6].

Adhesion layer is an amorphous blend of silicon with additional elements such as carbon and nitrogen. Silicon had selected as main material for adhesion layer because it is easily adheres to metal [7]. Adhesion layer required for overcoat because DLC layer does not sufficiently adhere to metal surface.

However, silicon works well to attach DLC so it is formed as silicon-carbon bond. Adhesion layer is formed as CSiC or CSiN. The function of adhesion layer is used to attach the DLC layer to the metal surface. Although silicon adheres well with carbon but it provides limited very thin silicon thickness will provide limited corrosion protection.

2.4 Corrosion

Corrosion is the electrochemical reaction between metal and environment. In thin film of magnetic layer, it contains metal materials. Corrosion can be occurred as galvanic corrosion. Galvanic corrosion is an electrochemical interaction of two or more materials having a sufficiently distinct galvanic potential difference.

In general, metal corrosion is oxidation in aqueous solution. The possible reaction for corrosion of thin film magnetic head can be representing reaction as shows in **Figure 2.6.**

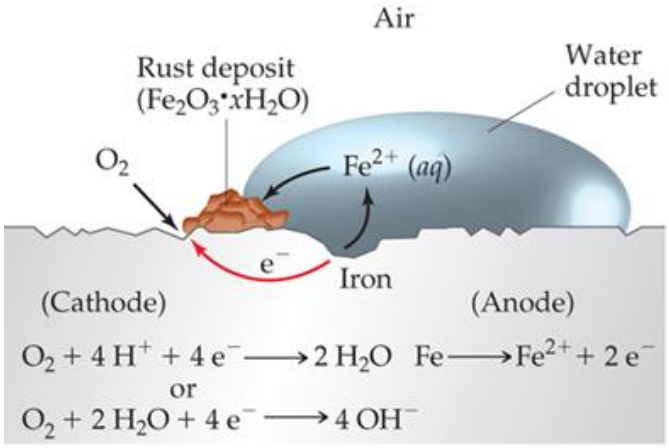

Figure 2.6 Reaction of galvanic corrosion [8].

2.5 Electrical Parameters

Read/write performance can be measured by electrical tester as parametric tests that characterize the fundamental parameters.

2.5.1 Clearance

Clearance is a space between top of media and slider surface when heater is turned on. **Figure 2.7** shows schematic of clearance.

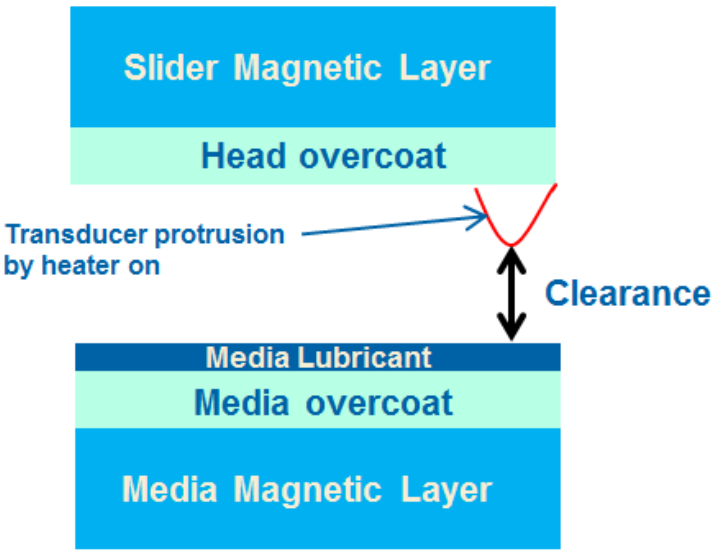

Figure 2.7 Schematic of clearance

Clearance measurement is measured by amplitude changing between passive fly (heater off) and heater induced contact (heater on). A schematic shows in **Figure 2.8**

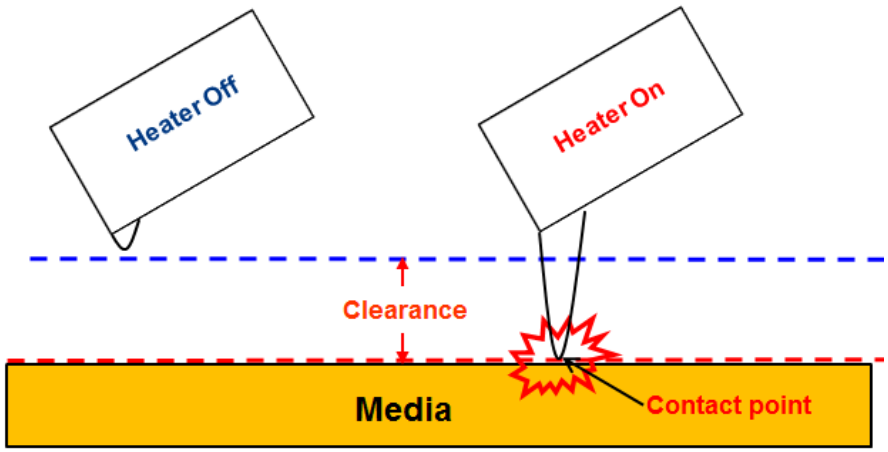

Figure 2.8 Schematic of clearance measurements

2.5.2 Amplitude

The amplitude of a recording system is characterized by writing single-frequency patterns and averaging the peak-to-peak amplitude of the read-back waveform around the track.

These measurements are referred to track-averaged amplitude (TAA). The most common measurements are “low frequency” (LFA) and “high frequency” (HFA). Amplitude average calculation is shown in equation (2.2),

Amplitude Average = Total amplitude of each cycle test / Number of cycle test (2.2)

where A is peak to peak

Amplitude measurement is shown in **Figure 2.9**

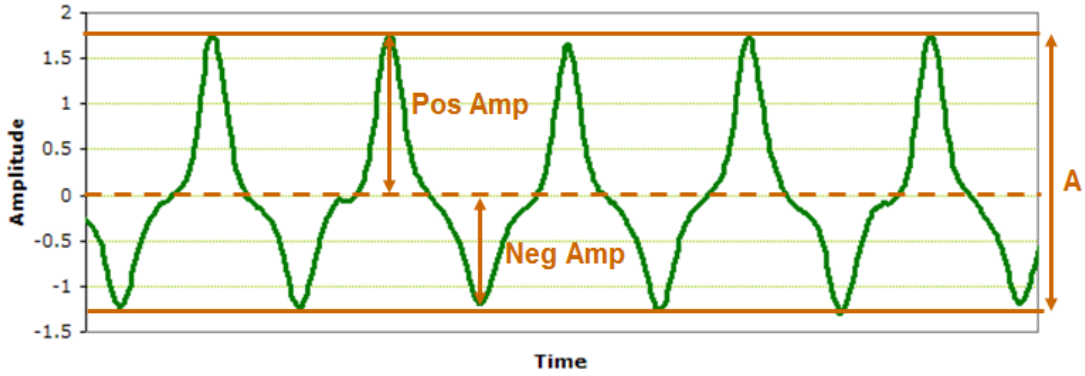

Figure 2.9 Amplitude Measurement

2.5.3 Overwrite (OVW)

In a hard disk drive, new data is written directly over old data, without erasing the old data. So overwrite is a characterization to show the ability of a writer to write over old data. Overwrite calculation is shown in equation (2.3),

OVW (dB) = 20*Log10 (residual HF fundamental / original HF fundamental) (2.3)

where HF is high frequency.

2.5.4 Bit error rate (BER)

For data transmission, it is possible for getting error in system especially for recording system as data transmission is noisy then the integrity of the system may be compromised.

Bit error rate (BER) is defined as errors occur in a transmission system. BER measurement is done by writing encoded data of known data as random sequence onto media. After that, data was read back to compare with written data sequence. The errors were counted as shown in equation (2.4),

$$\text{BER} = \text{bits errors detected/ total bits passed} \tag{2.4}$$

Since in hard disk drive, there is only as a small number of error occurs from many data patterns, BER is expressed as log value as shown in equation (2.5),

$$\text{BER} = \log(\text{bits errors detected/ total bits passed}) \tag{2.5}$$

2.6 Literature reviews

2.6.1 "The Head-Disk Interference Roadmap to an Areal Density of 4 Tbits/in^2" by M. B. Marchon *et al.* [1]

In 2013, M. B. Marchon *et al.* [1] reviewed "The Head-Disk Interference Roadmap to an Areal Density of 4 Tbits/in^2". Areal density (AD) in bits per square inch is the product of the linear density in bit per inch (BPI) and track density (TPI) as shown in equation (2.6),

$$\text{AD} = \text{BPI} \cdot \text{TPI} \tag{2.6}$$

Furthermore, the bit aspect ratio BAR is usually defined as

$$\text{BAR} = \text{BPI/TPI} \tag{2.7}$$

The head media spacing (HMS) have a very convenient expression linking HMS (in nm) to AD (in Tb/in^2), for a given BAR:

$$\text{HMS (nm)} \approx 15 \cdot (\text{AD} \cdot \text{BAR})^{-1/2} \tag{2.8}$$

Numerical HMS values based on (2.8) are reproduced in **Table 2.1.**

Table 2.1 Estimated HMS (nm) values as a function of AD and BAR.

	BAR			
AD (Tb/in^2)	3.0	3.5	4.0	4.5
2	6.2	5.8	5.4	5.1
4	4.4	4.1	3.8	3.6

As shown in **Table 2.1**, achieving a 4 Tb/in^2 areal density will require an HMS in the vicinity of ~4.4 nm. **Table 2.2** offers two scenarios for the HMS breakdown into its various components.

Table2.2 HMS breakdown scenarios for 4 Tb/in^2

HMS Budget	1 Tb/in^2			4 Tb/in^2			HMS adder	
Components	INSIC 2010	Target HMS by ~2014		INSIC 2010	Target HMS by ~2020-21		(effect of HAMR, BPM)	
Component		Hi	Lo		Medium risk	High risk	BPM	HAMR
TDH	1.8	2.0	1.0	1.4	1.1	0.6	0.3	0.5
Disc overcoat	0.9	2.5	2.0	0.6	1.8	1.5	0.3	0.6
Disk lubricant	0.9	1.2	1.0	0.8	1.0	0.8		
Clearance	1.3	1.2	1.0	0.6	0.6	0.5	0.2	0.3
Head overcoat	1.0	2.0	1.5	0.7	1.1	0.9		
Total	5.8	8.9	6.5	4.0	5.6	4.3	0.8	1.4

(I) **Disk and Head Overcoat**. It is clear from **Table 2.2** that the biggest contributor to HMS is the carbon overcoat, both on the disk and on the head. Historically, overcoat thickness reduction on both components has been enabled by denser carbon, as well as smoother underlying surfaces for the magnetic media and read/write elements (head). Head carbon has evolved from sputtered to plasma-enhanced chemical vapor deposition (PE-CVD) to filtered cathodic arc (f-CAC) carbon, which increased the density, sp3/sp2 ratio, and hardness. On the disk side are coated with some sort of PE-CVD deposited amorphous carbon overcoat. On the head side, evolutionary optimization of the overcoat technology might allow to reach the 4 Tb/in^2 goal of ~1 nm. Our estimate of such benefit is in the range of 0.2–0.3 nm or greater, for an overall reduction of ~0.5 nm. That is a substantial amount of about 10% of the total HMS.

(II) **Disk Lubricant**. **Table 2.2** shows that a 0.2 nm reduction of lubricant thickness from 1.0–1.2 to 0.8–1.0 is needed. This does not seem like much, but extremely tight reliability/HMS margins. This change is actually significant. It remains to be seen whether conventional lubricant chemistries (functionalized perfluoropolyether) will be able to achieve this thickness goal. Perhaps unconventional approaches, such as direct surface treatment/functionalization of the disk overcoat will be needed.

(III) **Touchdown height (TDH)**. Touchdown height (TDH) globally defines all residual disk and head topographies that prevent the head from coming into close proximity to the magnetic media. It is affected by waviness and roughness (<1 μm) of the substrate. TDH is not a requirement for proper HDD reliability and could, in theory, be brought to zero.

(IV) **Head-Disk Clearance**. Of all the HMS contributors, clearance has probably exhibited the largest decrease in the last 10 years. This revolutionary approach has allowed the HDD industry to achieve a 10-fold reduction in clearance from ca. 10 nm ten years ago to ～1.5 nm today (**Table 2.2**). To achieve the 0.6 nm, clearance goal and to easily compensate for clearance changes induced by temperature, altitude, or humidity, further enhancement of clearance control will be needed such as closed-loop control.

2.6.2 "Investigation of wear resistance and life time of diamond-like carbon (DLC) coated glass disk in flying height measurement process" by K. Phetdee *et al* [3].

In 2011, K. Phetdee *et al.* studied "Investigation of wear resistance and life time of diamond-like carbon (DLC) coated glass disk in flying height measurement process" They investigated durability and lifetime of the DLC coated glass disk in flying height measurement process. First, they studied about adhesion layer thickness as they found that the adhesion layer decreased the visibility of pole tips which it will be reference position in flying height tester. Then, they selected 5 thicknesses of

adhesion layer with 15 nm of DLC thickness that not decreased visibility of pole tip to investigate lifetime of DLC coating.

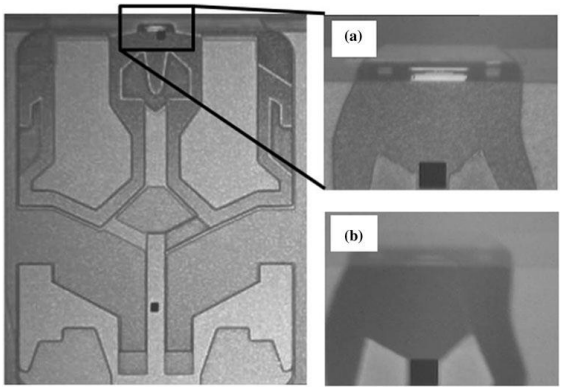

Figure 2.10 Position of pole-tip on slider a) shows pole-tip image captured through a commercial glass disk. b) glass disk coated with 9 nm thick silicon and 15 nm thick DLC [3].

Adhesion layer as various thickness with 15 nm of DLC were subjected to wear and visibility test. Wear test, triboindentor was used for testing and then wear profile were obtained by AFM. Visibility test and lifetime measurement were done in flying height tester which they do test until head scratch or wear appeared on disk surface. The result for wear resistance, they found that DLC overcoat significantly improved wear resistance and also wear depth decreased as compared with glass disk without DLC overcoat.

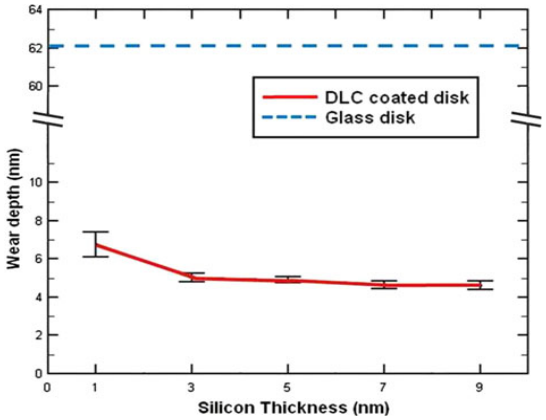

Figure 2.11 Average wear depths measured on the DLC coated disks as a function of silicon thickness. The dotted line represents the average wear depth measured on an uncoated disk [3].

Wear resistance is slightly increase with increment of adhesion layer but it's not significant while wear depth decreased with increment of adhesion layer. Visibility of pole tip will be poorer as thickness of adhesion layer increased. DLC overcoat disk improved lifetime as compared with glass disk without DLC overcoat.

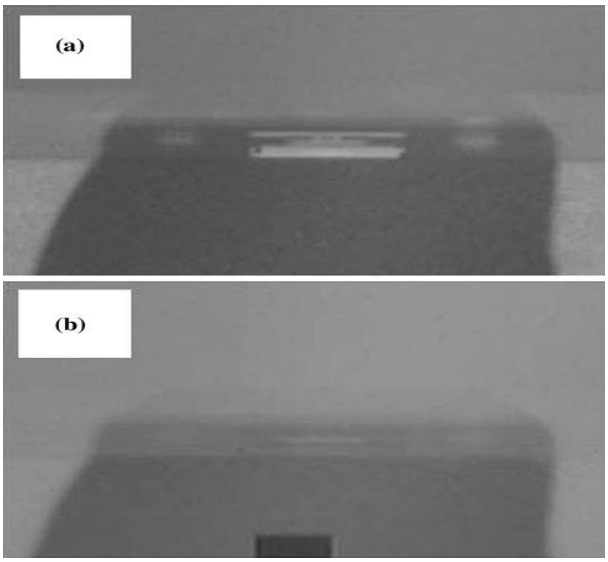

Figure 2.12 Pole-tip images captured through: a) the coated disk (3-nm Si/15-nm DLC) and b) the other coated disk (9-nm Si/15-nm DLC [3].

2.6.3 "Adhesion Layer For Protective Overcoat" by C. Fang *et al.* [4]

In 2011, C. Fang *et al.* [4] developed "Adhesion Layer For Protective Overcoat". An amorphous adhesion layer on metal substrate and a protective DLC layer over the adhesion layer. The adhesion layer has thickness less than 8 Å with composition of carbon silicon carbide or carbon silicon nitride. The composition of adhesion layer provides corrosion resistance for metal substrate. **Figure 2.12** is schematic of portion of slider.

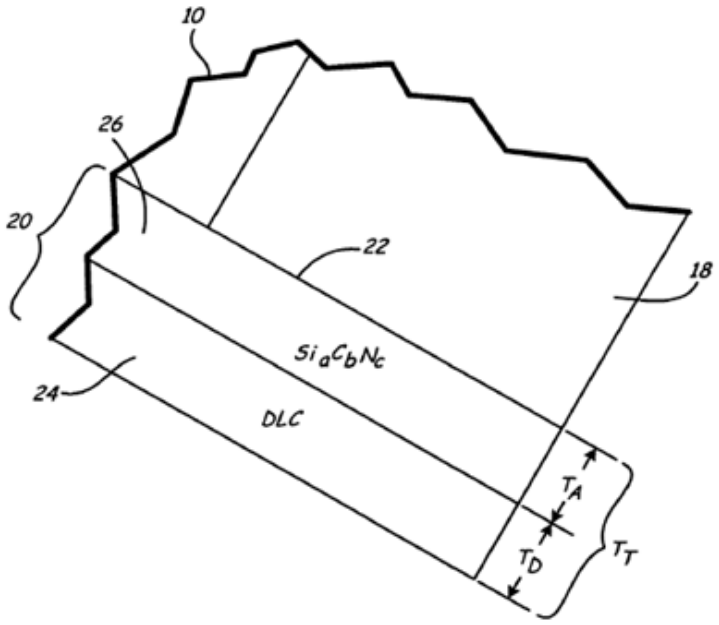

Figure 2.13 Schematic of portion of slider [4].

Protective overcoat (20) is applied to surface (22) of slider. Primary functions of overcoat are to protect against wear and corrosion. In particular, it is important to protect the exposed metal parts of transducer (18). Diamond like carbon (24) preferred for protective overcoat due to high hardness, high wear resistance, low coefficient of friction and chemical inertness. Adhesion layer (26) used silicon as main component. Silicon is easily to adhere to metal when deposited on metal surface. The silicon reacts with surface and form silicide. Thus, adhesion layer formed primarily of silicon, adhesion would adhere well on metal surface. Moreover, diamond like carbon (DLC) adheres well to silicon as forming silicon-carbon bond. However, silicon contributes minimal corrosion resistance to overcoat because diffused into surface then required more silicon to be deposited on metal surface. Alternatively, the overall thickness of overcoat may remain similar in thickness to current overcoat design, yet exhibit greater corrosion resistance. Adhesion layer is an amorphous blend of silicon with additional components but not limited to carbon and nitrogen. Adhesion layer is labeled as $Si_aC_bN_c$ where a, b and c represent compositional range of each element in atomic percent.

In another embodiment, adhesion layer is formed of silicon and carbon. Adhesion layer may be formed from target of silicon carbide blended with additional

carbon, resulting in carbon silicon carbide (CSiC). In another embodiment, adhesion layer is formed of carbon silicon nitride (CSiN). When adhesion layer is an amorphous blend of silicon mixed with second or third element, adhesion layer exhibit significant advantage. Moreover, there is minimal diffusion of silicon to surface. Due to the unique composition of adhesion layer, it is possible for protective overcoat to be thinner compare to current configuration of protective overcoat. Head media spacing is reduced as reduction of total thickness of overcoat. An additional benefit of adhesion layer is its improved oxidation resistance. To achieve thinner overcoat to reduced HMS range of adhesion layer is 4 to 10 Å and DLC layer is 7 to 15 Å. Adhesion layer may be formed using unknown thin film deposition technique but not limited to evaporation, sputtering or plasma deposition. Commonly, adhesion layer is deposited onto surface by physical vapor deposition.

CHAPTER 3

RESEARCH METHODOLOGY

This chapter describes reliability characterization of head overcoat (HOC). Corrosion, read/write performance, topography and wear behaviors were evaluated. High accelerated stress tests (HAST) to characterize corrosion were performed on HGA based on 3 different HOC thicknesses. Read/write performance was evaluated in terms of a change in electrical parameter due to stress burnishing using spin-stand tester. Topography was characterized after electrical measurement by atomic force microscopy (AFM). Last, wear on pole tip was observed by field-emission electron microscopy (FESEM).

3.1 Design of HOC Thickness

Four techniques were used to investigate effect of HOC thickness on reliability. There are three types of HOC thickness were used in this study; 16 Å, 20 Å and 24 Å. **Figures 3.1** and **3.2** show schematic views of HOC structure and HOC details of each HOC thickness, respectively. **Table 3.1** shows details of HOC for each thickness.

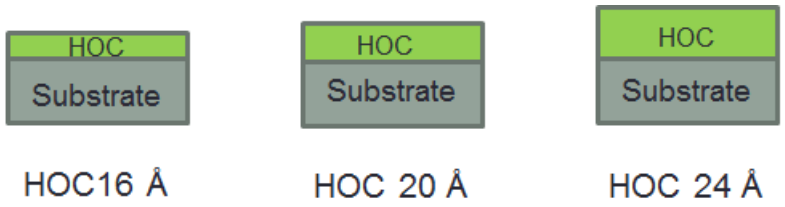

Figures 3.1 Schematic view of HOC structure

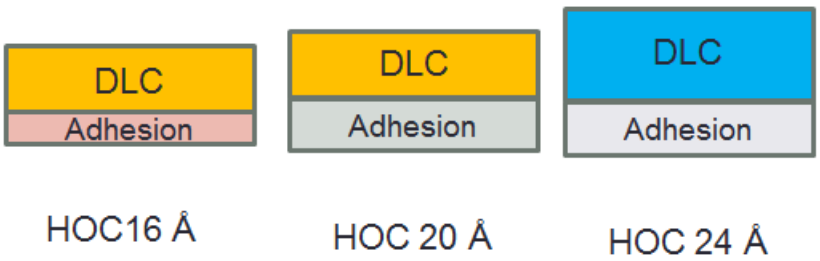

Figures 3.2 Details of HOC for each thickness

Table 3.1 The details of HOC for each thickness

Details of HOC	HOC 16 Å	HOC 20 Å	HOC 24 Å
Adhesion type	A	A	B
Adhesion layer thickness	<Y	Y	Y
DLC type	C	C	D
DLC layer thickness	X	X	>X

3.2 Corrosion Characterization by High Accelerated Stress Test (HAST)

High accelerated stress test (HAST) was used to characterize corrosion behavior which may be directly influenced by thin HOC layer.

HAST is a technique that applies stress test on HGA to stimulate corrosion. HGA was tested in HAST chamber (EHS - 411MD ESPEC) and subsequently observed by field emission scanning electron microscope (FESEM) (Hitachi S4800-II). In HAST chambers, severe environment was created to accelerate early corrosion on HGA. FESEM was used to capture image of corrosion after HAST. The test procedure is as follows.

Step 1: Preparation of HGA for HAST. 4 HGAs were prepared for each HOC thickness. The conditions for HAST were controlled under elevated temperature, high humidity for designated hours. **Figure 3.3** shows a photo of HAST chamber.

Figure 3.3 Photo of HAST Chamber (EHS - 411MD ESPEC) [www.espec.co.jp]

Step 2: FESEM characterization. After HAST, HGAs were characterized by FESEM for corrosion measurement. Standard condition for FESEM observation was magnification of 2.0 kX and an accelerated voltage of 2.0 kV. **Figures 3.4** and **3.5** show photos of FESEM machine and an example of FESEM image of HGA after HAST, respectively.

Figure 3.4 Photo of FESEM (Hitachi S4800-II)

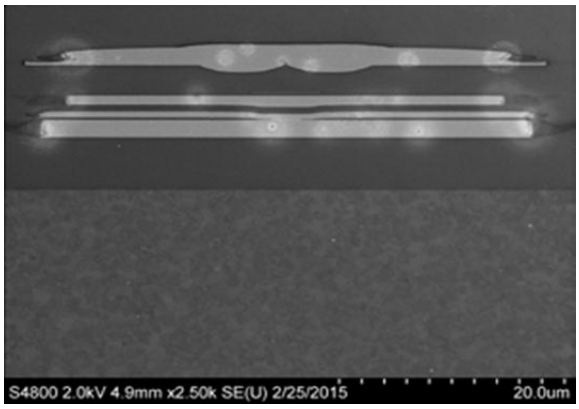

Figure 3.5 Example of FESEM image of HGA after HAST

Step 3: FESEM image was used for corrosion analysis. Bright needle and spot will be considered as corrosion. Corrosion position will be counted and determined as the failure if it is not in the acceptable range.

3.3 Read/Write Performance Characterization

To investigate read/write performance of each HOC thickness, electrical measurement was done on spin-stand tester for reliability test with stressed burnishing. **Figure 3.6** shows a photo of spin-stand tester.

Figure 3.6 Photo of spin-stand testers

The test algorithm is dwelling the head interference by stepping clearance level from +1 nm to -4 nm with a step size of 0.5 nm and monitoring degradation of electrical performance at each interference level. The test procedure is as follows.

Step 1: Preparation of HGA for electrical measurement on spin-stand tester. 15 HGAs were prepared for each HOC thickness.

Step 2: Characterization by spin-stand tester.

2.1: Measure clearance performance for head screening. Head will be moved to next step, if it passes criteria for clearance performance screening. Output from this step provides clearance (nm) and power to contact; PtC (mW) data.

2.2: Calculate fixed power for electrical parameters testing. Fixed power was used for head flying at read/write target for electrical measurement.

2.3: Measure electrical parameters. In this study focused on electrical parameters as

- **Clearance**: Space between top of media and slider surface.
- **Power to contact (PtC):** Total power that been used since head start to protrude until contact media.
- **Overwrite (OVW):** Ability of a writer to write over old data.
- **Bit error rate (BER):** Ratio between error bit detected and total bit passed.
- **Amplitude (AMP):** Averaged of read back signal.
- **Reader resistance (RD_RES):** is the property of a reader to change the value of its electrical resistance.

All electrical parameters were measured at reference track on fly height target. Output from this step was used as reference data and was used to compare with other data from difference interference in latter step.

2.4: Move head to dwell track for stress burnishing at dwell interference level starting from +1 nm. Dwell power for burnishing was calculated based on PtC.

2.5: Move head back to reference track again and electrical parameters at read/write target were measured. At this step, the electrical parameters were measured again and compared with reference data to estimate degradation rate. Degradation rate is delta of electrical parameters

between data after interference and reference data. The degradation of each parameter calculated as follows.

Delta Clearance (nm):

Clearance at interference level –reference clearance (2.1)

Delta PtC (mW):

PtC at interference level – reference PtC (2.2)

Delta BER (dcd):

BER at interference level – reference BER (2.3)

Delta OVW (dB):

OVW at interference level – reference OVW (2.4)

Delta RD_RES (%):

{(RD_RES at interference level – reference RD_RES)/ reference RD_RES} *100 (2.5)

Delta AMP (%):

{(AMP at interference level – reference AMP)/ reference AMP} *100 (2.6)

2.6: Increase interference level with step size of 0.5 nm and then repeat steps 2.4 and 2.5 until dwell interference reaching -4 nm. **Figure 3.7** shows flow of test algorithm.

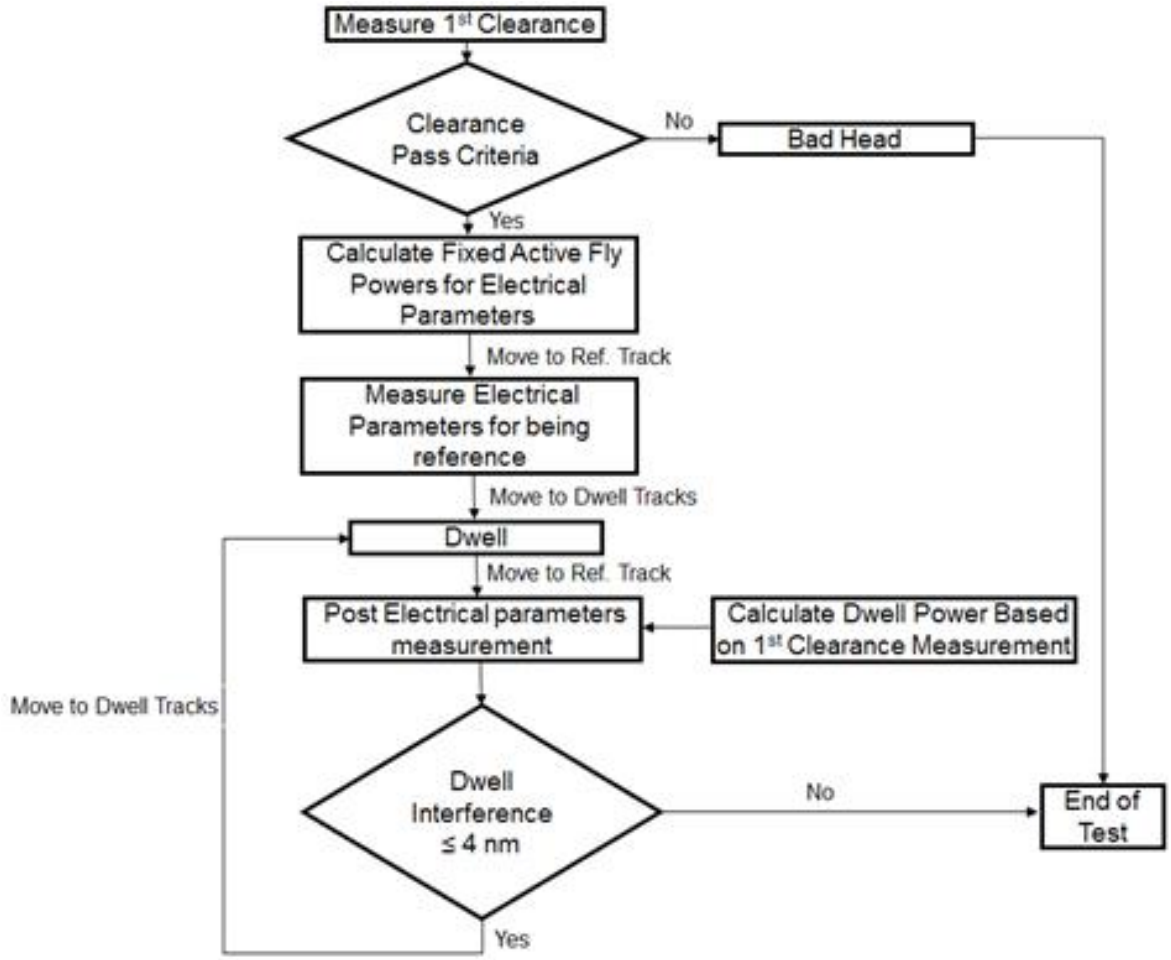

Figure 3.7 Flow of test algorithm

Step 3: Analyze the data by JMP software. **Figure 3.8** shows a photo of a screen of JMP software.

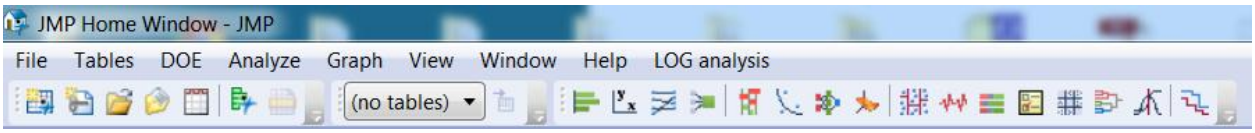

Figure 3.8 Photo of a screen of JMP software

Analysis procedure by JMP software is as follows.

3.1: Open excel file that containing all electrical data to transform to JMP file for analyze. **Figure 3.9** shows example data on JMP software.

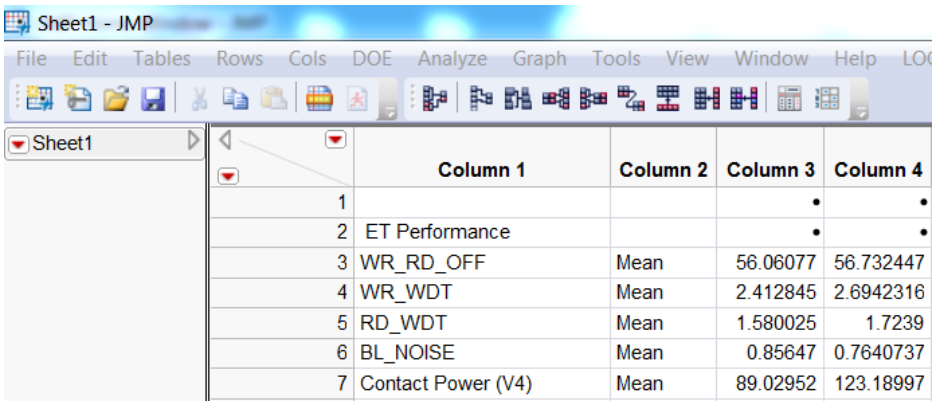

	Column 1	Column 2	Column 3	Column 4
1			•	•
2	ET Performance		•	•
3	WR_RD_OFF	Mean	56.06077	56.732447
4	WR_WDT	Mean	2.412845	2.6942316
5	RD_WDT	Mean	1.580025	1.7239
6	BL_NOISE	Mean	0.85647	0.7640737
7	Contact Power (V4)	Mean	89.02952	123.18997

Figure 3.9 Example data on JMP software

3.2: Analyze electrical data before burnishing. These data were used to confirm read/write performance before burnishing by Tabulate function. **Figure 3.10** shows a photo of a screen of Tabulate function.

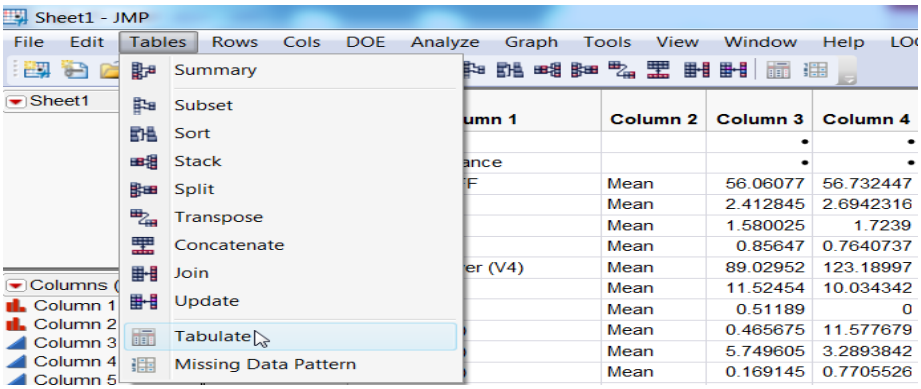

Figure 3.10 Photo of a screen of Tabulate function

3.3: Read out electrical data from Tabulate before burnishing. **Figure 3.11** shows example of result from Tabulate function.

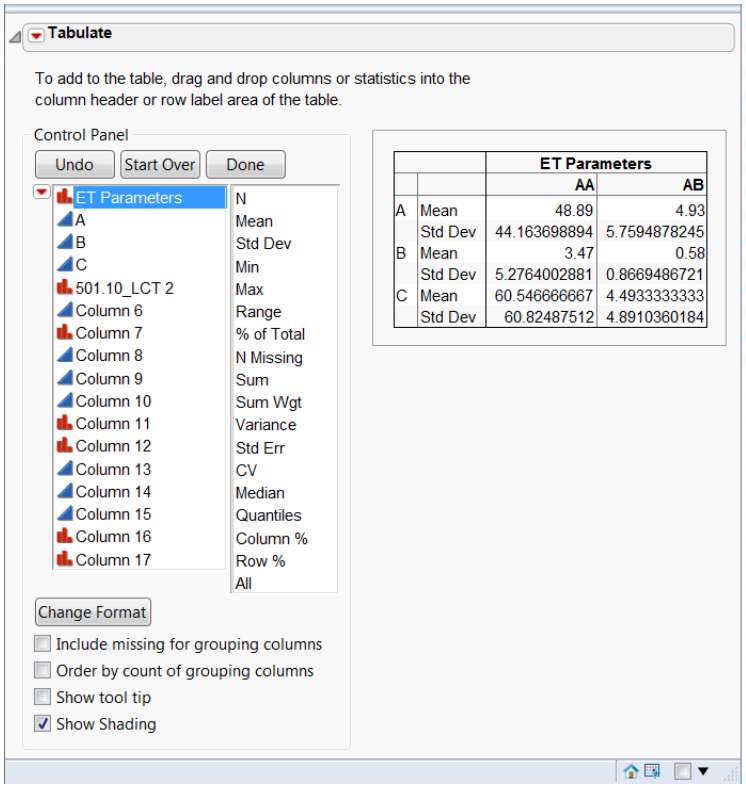

Figure 3.11 Example of result from Tabulate function

3.4: Plot the graph using function; Analyze (Fit Y by X). **Figure 3.12** shows a photo of a screen of Analyze function.

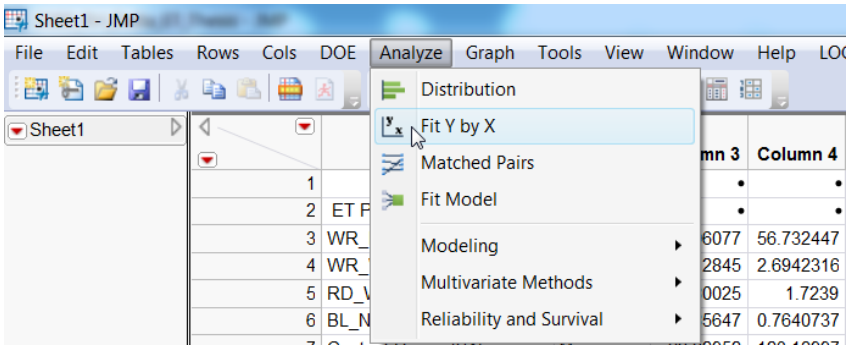

Figure 3.12 Photo of a screen of Analyze function

3.5: Select all electrical parameters for plotting as Y-axis is electrical parameters and X-axis is interference level. **Figure 3.13** shows a photo of a screen of Fit Y by X function.

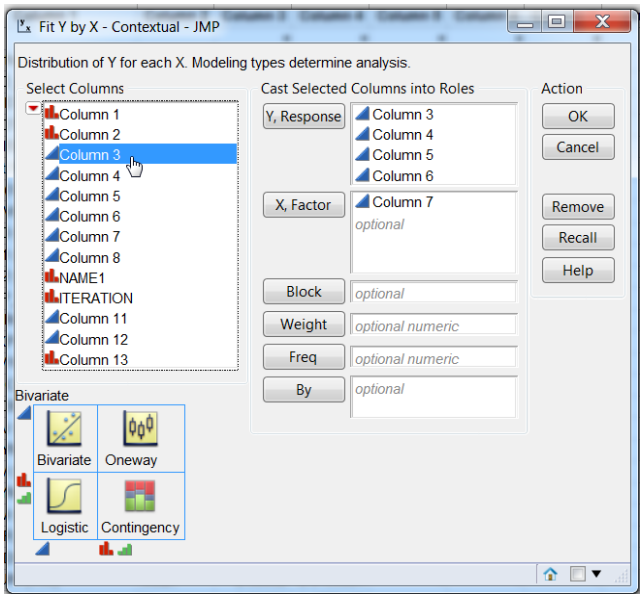

Figure 3.13 Photo of a screen of Fit Y by X function

3.6: Select "Group By" for grouping the data to analyze. **Figure 3.14** shows example for data grouping.

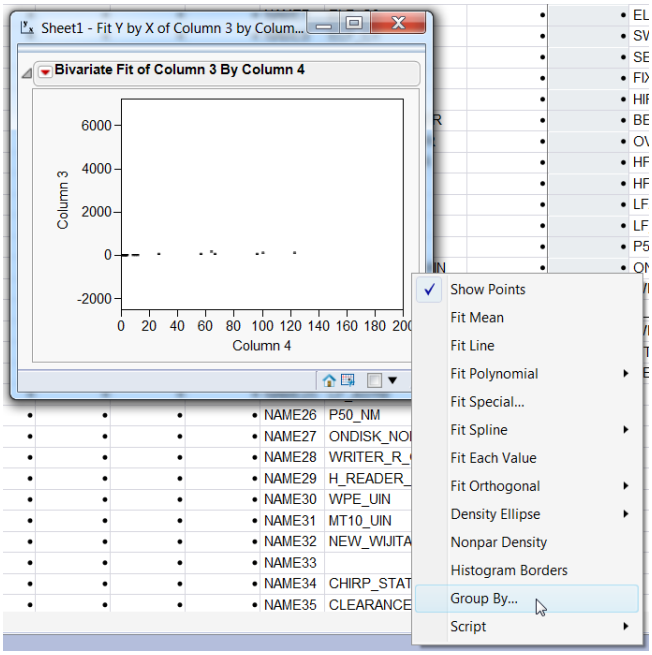

Figure 3.14 Example of data grouping

3.7: Plot all electrical parameters. The data were separated for each HOC thickness. **Figure 3.15** shows example of final plotting graph

.

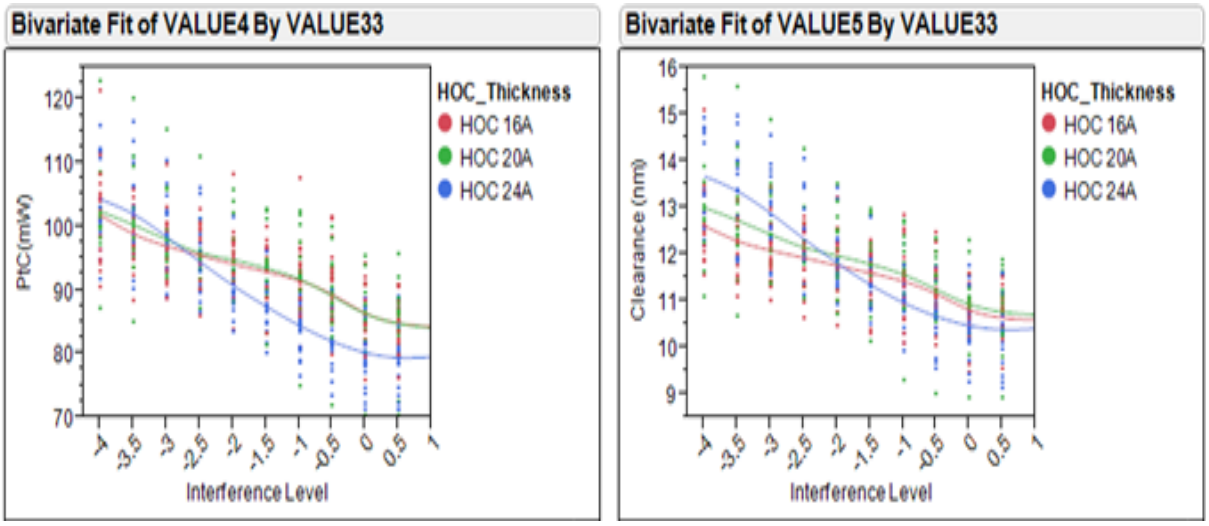

Figure 3.15 Example of final graph plotting

3.4 Topography Characterization

Topography was characterized by atomic force microscope (AFM) after read/write process. **Figure 3.16** shows a photo of AFM (BRUKER; Dimension Icon).

Figure 3.16 Photo of AFM (BRUKER; Dimension Icon)

The test procedure on spin-stand tester is as follows.

Step 1: Sample preparation. After electrical measurement, the same sample was further characterized by AFM.

Step 2: AFM measurement conditions is as follows.

AFM mode : Tapping mode

Scan size : 60 μm x 60 μm

Scan angle : 0°

Scan rate : 0.4 Hz

Step 3: Image analysis by “Nano Scope Analysis” software.

3.1 Open “Nano Scope Analysis” software. **Figure 3.17** shows a photo of a screen of “Nano Scope Analysis” software.

Figure 3.17 Photo of a screen of “Nano Scope Analysis” software

3.2 Open file for analysis. File type is .001 file. **Figure 3.18** shows a photo of file selection for analysis

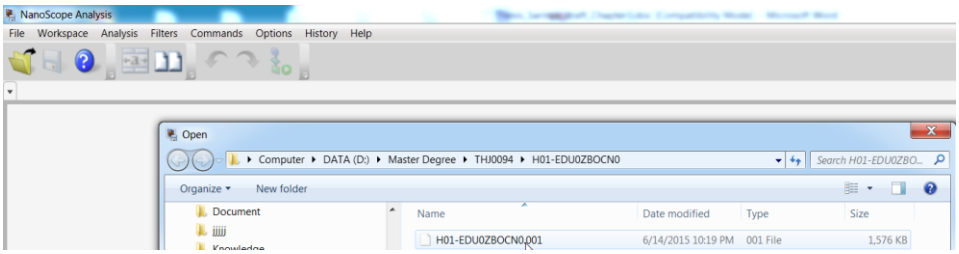

Figure 3.18 Photo of file selection for analysis

3.3 Start to analyze by select “High sensor” tab. **Figure 3.19** shows a photo of selected image for analysis.

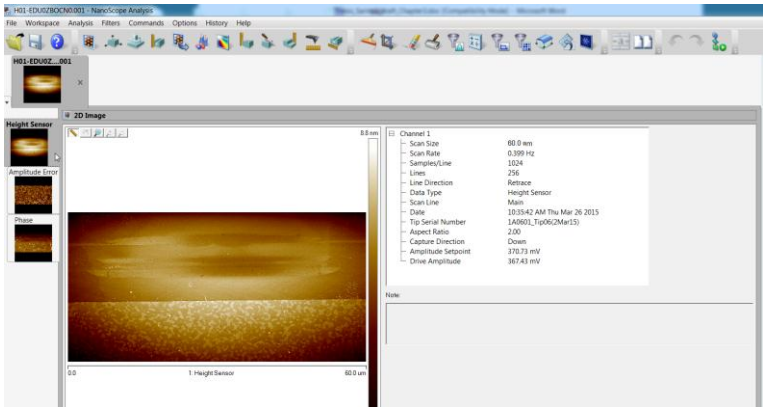

Figure 3.19 Photo of selected image for analysis

3.4 Flatten image with 2nd order for clearly imaging. **Figure 3.20** shows a photo of a screen of image flattening. **Figure 3.21** shows a photo of an image after flattening which is clearer.

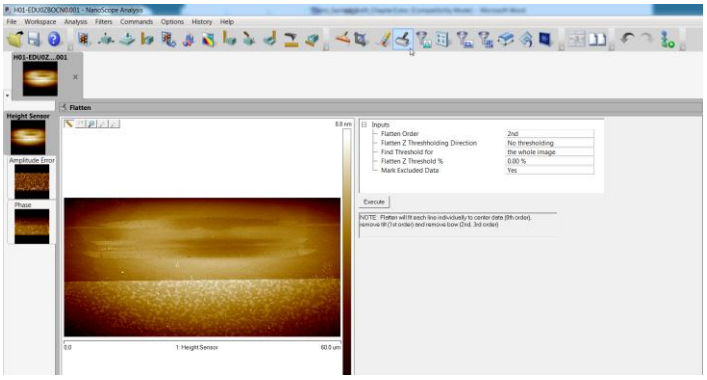

Figure 3.20 Photo of a screen of image flattening

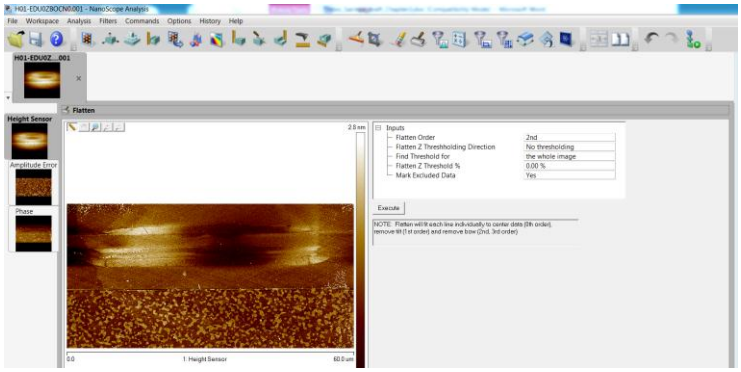

Figure 3.21 Photo of an image after flattening

3.5 Show 3D image by “3D Image” function. **Figure 3.22** shows an example of 3D image of HGA.

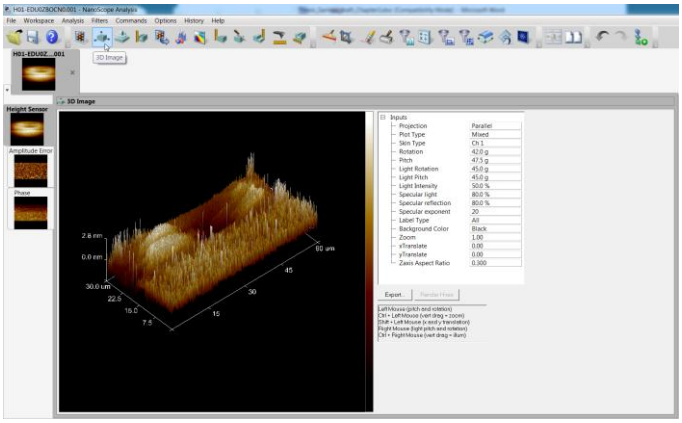

Figure 3.22 An example of 3D image of HGA

Step 4: Analyze depth by “Seaware” software.

4.1 Open “Seaware” software. Figure 3.23 shows a photo of a screen of “Seaware” Software.

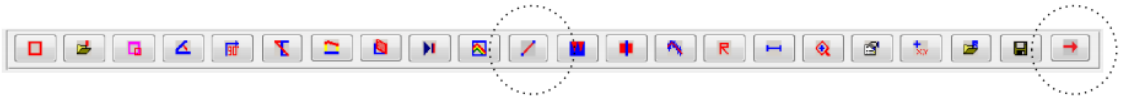

Figure 3.23 Photo of a screen of “Seaware” Software

4.2 Open file for analysis. File type is .001 file. Interest area was selected for analysis. **Figure 3.24** shows a photo of interest area for analysis.

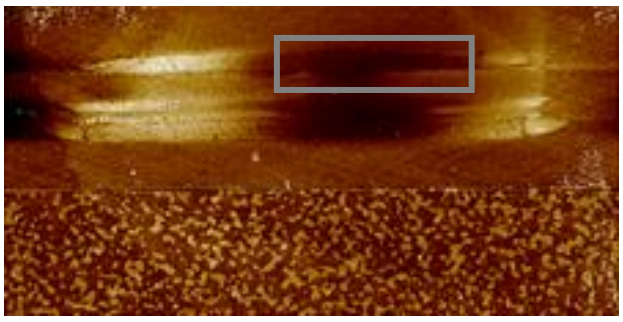

Figure 3.24 Photo of interest area for analysis.

4.3 Select  to obtain line profile of selected area. Drag a line from left to measure wear **Figure 3.25** shows a photo of line profile of selected area.

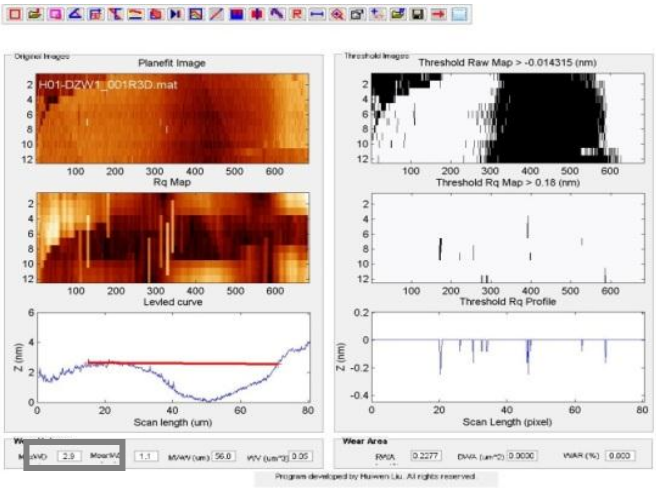

Figure 3.25 Photo of line profile of selected area

3.5 Wear Characterization

Wear on transducer that occurred from electrical measurement process was observed by FESEM.

Step 1: FESEM test sample is the same sample for electrical and AFM measurements. **Figure 3.26** shows a photo of FESEM (Carl Ziess; Ultra 55).

Figure 3.26 Photo of FESEM (Carl Ziess; Ultra 55)
[http://rusnanonet.ru/nns/29470/equipment/?page=35149]

Step 2: Observe wear on pole tip area under FESEM magnification and accelerated voltage of 2.2 kX and 1.0 kV, respectively. **Figure 3.27** shows example of FESEM image.

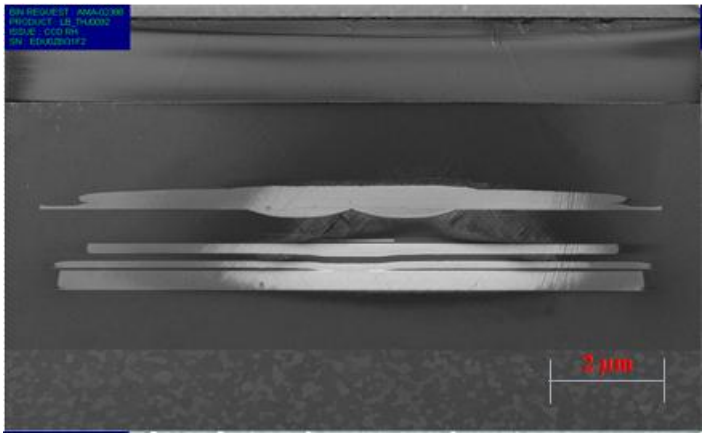

Figure 3.27 Example of FESEM image

Step 3: Select output of FESEM image as TIF file.

Step 4: Analyse wear area by Quartz PCI software.

4.1 Open “Quartz PCI” software. **Figure 3.28** shows a photo of a screen of “Quartz PCI” software.

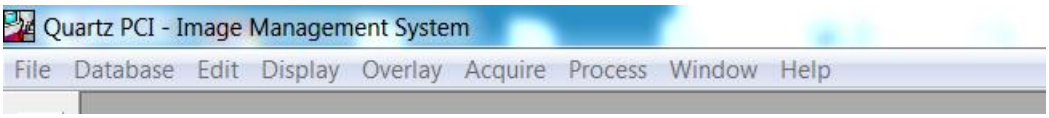

Figure 3.28 Photo of a screen of “Quartz PCI” software.

4.2 Import file for analysis. File type is TIF file. **Figure 3.29** shows a photo of a screen of file selection for analysis.

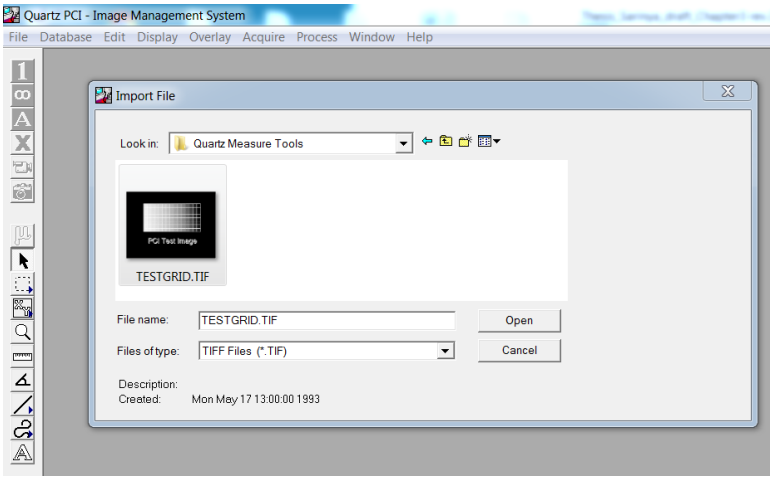

Figure 3.29 Photo of a screen of file selection

4.3 Start to analyze by select “Measuring tool” tab. **Figure 3.30** shows a photo of a screen of “Measuring tool” for analysis.

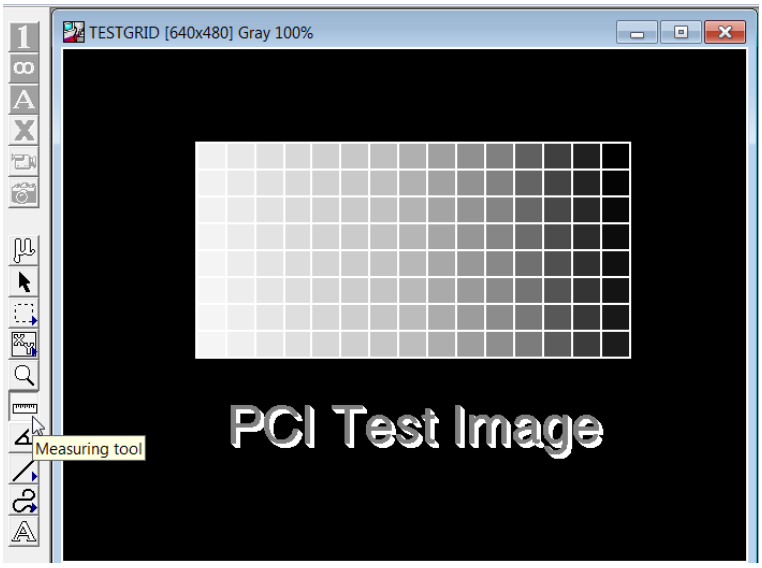

Figure 3.30 Photo of a screen of “Measuring tool”

4.4 Drag a reference line. **Figure 3.31** shows a photo of a reference line.

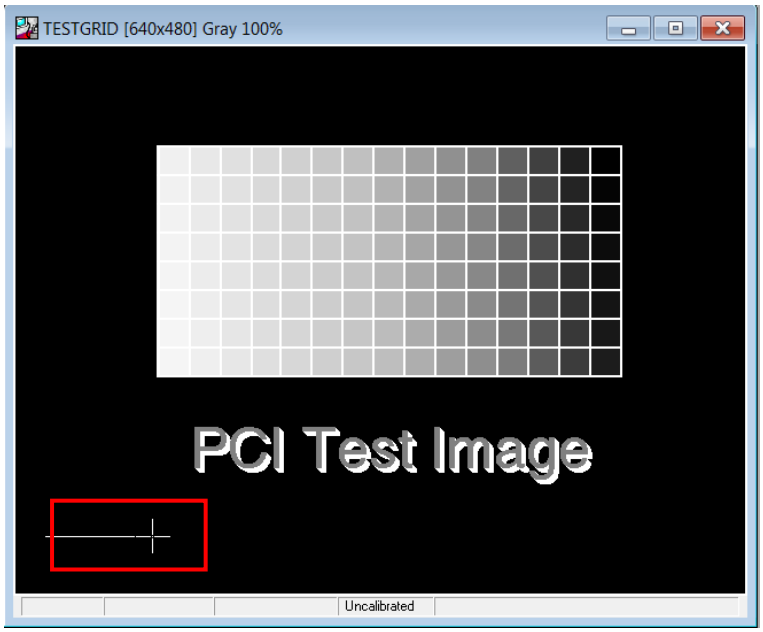

Figure 3.31 Photo of a reference line

4.5 Calibrate reference line. Fill information in a distance box and click calibrate. **Figure 3.32** shows a photo of a screen of calibrate box.

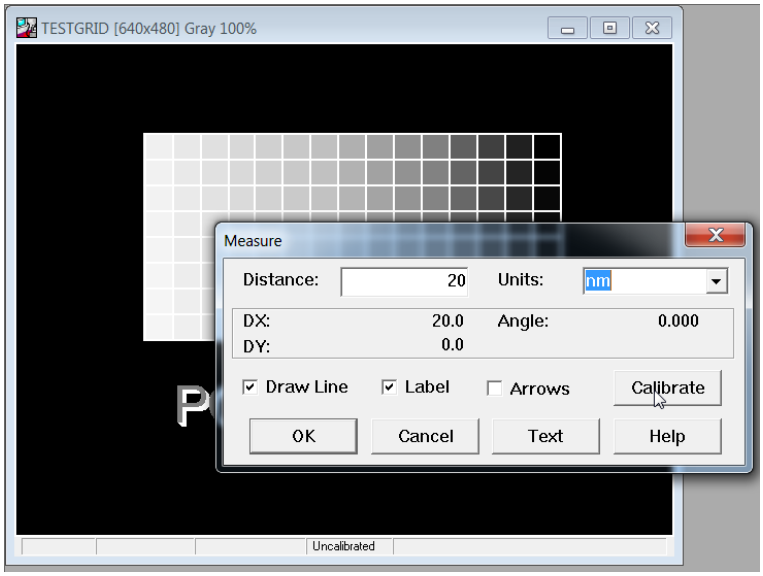

Figure 3.32 Photo of a screen of calibrate box

4.6 Select area for analysis by dragging line for x and y axis. **Figure 3.33** shows a photo of selected area.

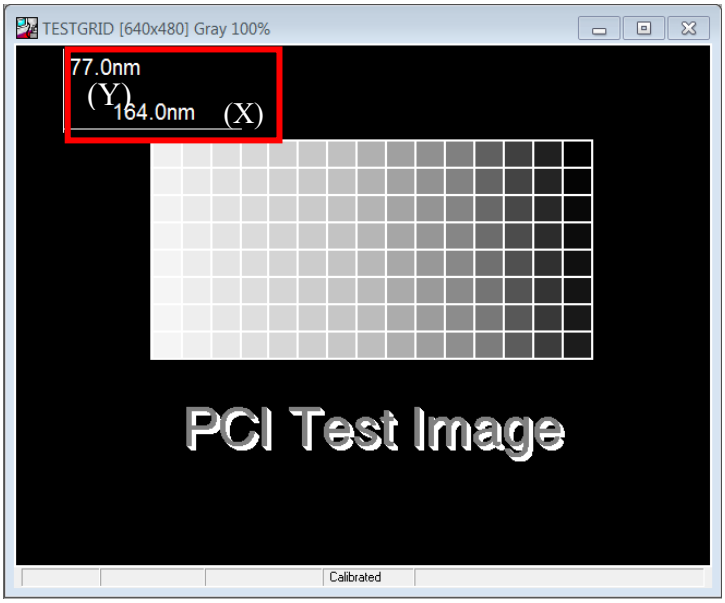

Figure 3.33 Photo of selected area

4.7 Calculate wear area by multiplying width (Y) and length (X).

CHAPTER 4

RESULTS AND DISCUSSION

This chapter describes the results of head reliability of various HOC thicknesses. High accelerated stress test (HAST), spin-stand tester, atomic force microscopy (AFM) and field emission scanning electron microscopy (FESEM) were used for corrosion, read/write performance, topography and wear resistance characterization, respectively. Effect of HOC thickness on its reliability was studied based on the characterization results.

4.1 Effect of HOC thickness on corrosion behavior

First, corrosion on pole tip area was observed. The head was treated by highly accelerated stress test (HAST) under condition shown in 3.2.1.

After HAST, head was characterized by field-emission scanning electron microscopy (FESEM) to observe corrosion behavior. **Figure 4.1** shows FESEM image of head around pole tip area before HAST. Head around pole tip area consists of writer and reader part.

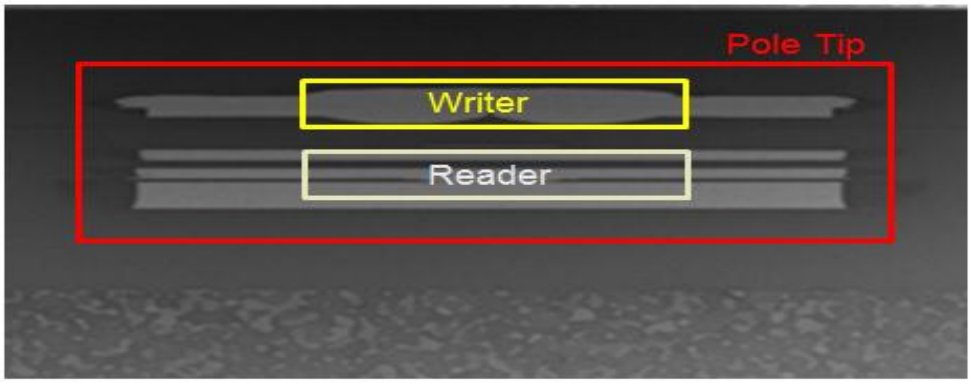

Figure 4.1 FESEM Image around pole tip area before HAST

The corrosion was determined by the bright spot on the head from FESEM image.

Figure 4.2 shows FESEM images of HOC 16 Å after HAST.

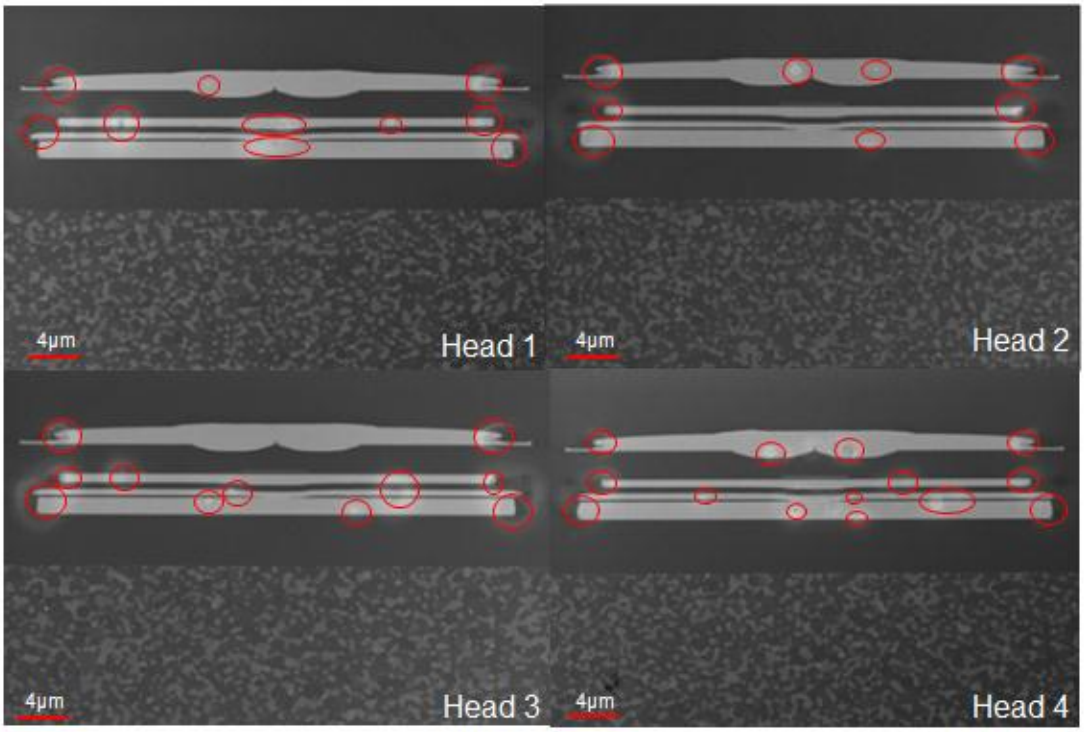

Figure 4.2 FESEM images of head with HOC 16 Å after HAST

A bright needle shape or spot was considered as corrosion and it was marked as red circle in the FESEM image. There are corrosion occurred on heads 1, 2, 3 and 4 for 10, 9, 11 and 14 positions, respectively. The positions of corrosion of heads 1 and 3 were near reader and the end of pole while head 2 and 4 were near the end of pole, writer and reader areas. The defect appearance is severe as its moderate brightness. However, it was considered as non-failure of corrosion as a number of corrosion positions are in acceptable range.

Figure 4.3 shows FESEM images of HOC 20 Å after HAST.

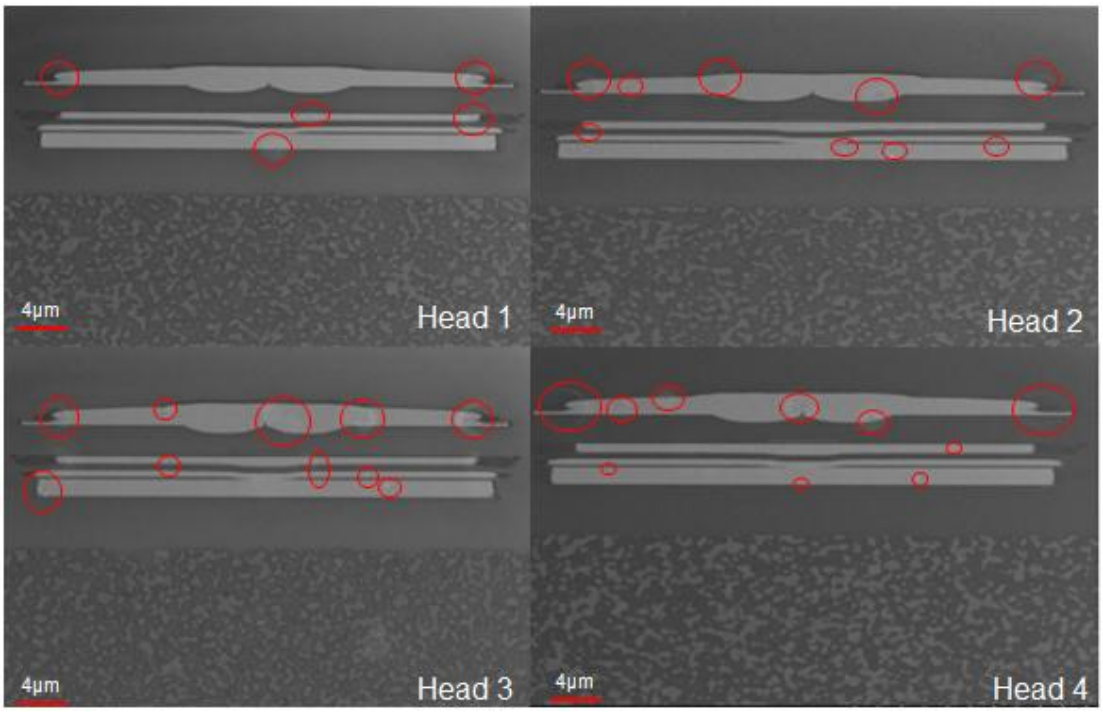

Figure 4.3 FESEM images of head with HOC 20 Å after HAST

There were bright spots appeared around pole tip area for all heads and they were considered as corrosion. There are defects occurred on heads 1, 2, 3 and 4 for 5, 9, 10 and 10 positions, respectively. The position of defects occurred on heads 1, 3, 4 is near the end of pole and reader area, while that of head 2 is near the end of pole, writer and reader areas. The defect appearance is non-severe as its less brightness. However, it was considered as non-failure of corrosion as a number of corrosion positions are in acceptable range it's in acceptable range.

Figure 4.4 shows FESEM images of HOC 24 Å after HAST.

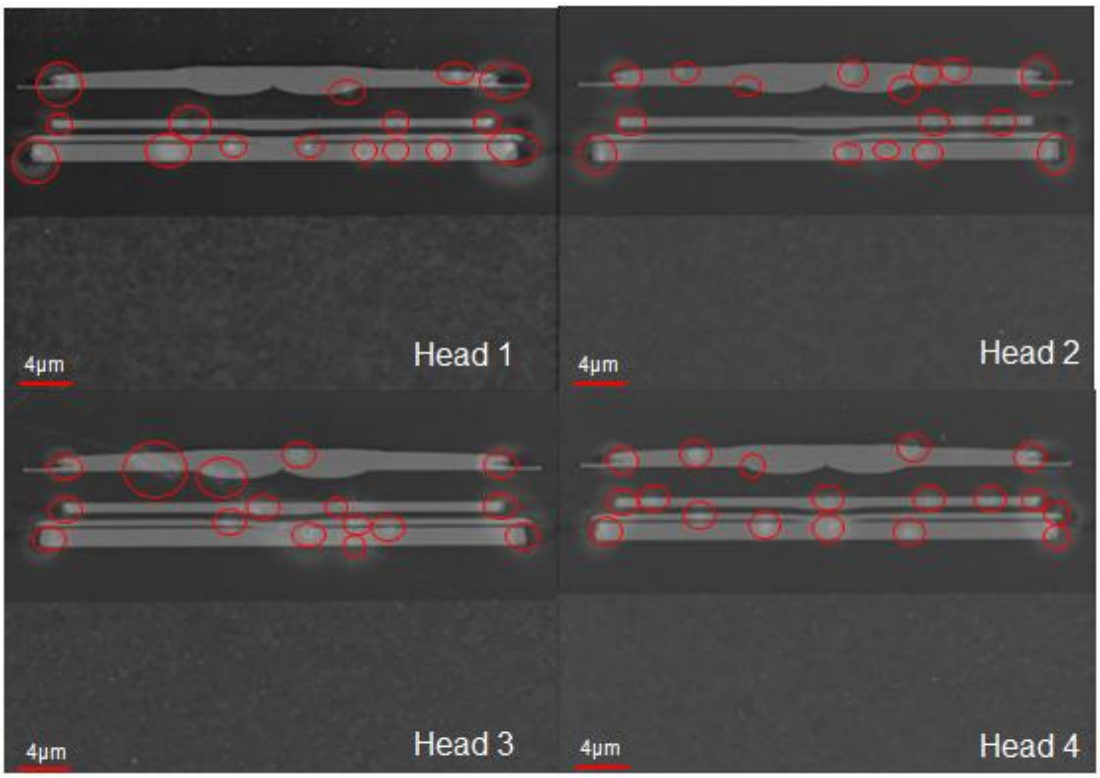

Figure 4.4 FESEM images of head with HOC 24 Å after HAST

There were bright spots appeared around pole tip area for all heads and they were considered as corrosion. There are defects occurred on heads 1, 2, 3 and 4 for 16, 16, 16 and 18 positions, respectively. The position of corrosion of heads 1, 2, 3 and 4 were near the end of pole, writer and reader areas. The defect appearance is severe as its high brightness. However, it was considered as non-failure of corrosion as a number of corrosion positions are in acceptable range it's in acceptable range.

The results of corrosion characterization of three types of HOCs can summarize as follows;

(1) HOC 24 Å (adhesion layer type B and DLC type D) shows the most severe corrosion. HOCs 16 (adhesion layer type A and DLC type C) and 20 Å (adhesion layer type B and DLC type C) show relatively same level of corrosion.

(2) DLC effects on corrosion behaviors. Despite its highest thickness, HOC 24 Å shows the highest brightness and area of corrosion positions, while HOC 20 Å shows the least brightness and area. According to HOC coating condition of

each head, HOCs 16 and 20 Å were prepared by the machine with small standard deviation but different HOC thicknesses, while HOC 24 Å was prepared by another machine with high standard deviation of film thickness and film uniformity. Due to the high standard deviation, there is high possibility of gap/hole formation on DLC film type D, leading to oxidation reaction between oxygen molecule and magnetic layer and resulting in corrosion.

The corrosion reaction can be expressed as follows;

$$4M\,(s) \longrightarrow 4M^{2+}(aq) + 8e^{-} \quad (4.1)$$

$$2O_2(g) + 4H_2O\,(l) + 8e^{-} \longrightarrow 8OH^{-}(aq) + 8e^{-} \quad (4.2)$$

$$4M^{2+}(aq) + 8OH^{-}(aq) \longrightarrow 4M(OH)_2\,(s) \quad (4.3)$$

$$4M(OH)_2\,(s) + O_2(g) \longrightarrow 2M_2O_3{\cdot}2H_2O\,(s) + 2H_2O(l) \quad (4.4)$$

where M is metal element of magnetic layers and $2M_2O_3{\cdot}2H_2O$ (s) is corrosion product.

However, all HOC thicknesses show a number of corrosion positions in acceptable range, thus it is not significant failure of corrosion.

4.2 Effect of HOC thickness on read/write performance

Normally, thin HOC provides poor reliability because transducer can be damaged easily than thick HOC. Thus, it is necessary to study read/write performance of thin HOC.

Electrical measurement is utilized to confirm read/write performance by the condition described in 3.2.2. First, electrical measurement before head burnishing was conducted as reference data. Read/write performances parameters are bit error rate (BER), overwrite (OVW), amplitude and reader resistance (RD_RES). Moreover, flying output which are power to contact (PtC) and clearance were also characterized.

Power to contact (PtC) is a power that head required for protrusion to make a contact with media. The power to contact of HOCs 16, 20 and 24 Å are 85.14, 82.52

and 79.74 mW, respectively. The power to contact value is inversely proportional to HOC thickness. The thinnest HOC, namely the widest head media spacing, requires the highest power to contact.

Clearance is a gap between top of media and slider surface when heater is turned on. The clearance of HOCs 16, 20 and 24 Å are 10.69, 10.51 and 10.42 nm, respectively. The clearance is inversely proportional to HOC thickness but proportional to the power to contact. The thinnest HOC, namely the widest head media spacing, provides the highest clearance.

Bit error rate (BER) is the number of bit errors per unit time to determine read ability of the head. The BER of HOCs 16, 20 and 24 Å are -2.13, -2.25 and -2.23 decade, respectively. Since all HOCs were fabricated from the same wafer, thus their BERs are relatively same value.

Overwrite (OVW) is ability of a writer to write over old data. The OVW of HOCs 16, 20 and 24 Å are -35.08, -36.35 and -36.29 dB, respectively. Since all HOCs were fabricated from the same wafer, thus their OVW are relatively same value.

Amplitude (AMP) is characterized by writing single-frequency patterns and averaging the peak-to-peak amplitude of the read-back waveform around the track. The AMP of HOCs 16, 20 and 24 are 13,727, 16,185 and 13,415 μV, respectively. Since all HOCs were fabricated from the same wafer, thus their AMP is relatively same value.

Reader resistance (RD_RES) is a resistance of reader stack. The RD_RES of HOCs 16, 20 and 24 Å are 266, 248 and 214 Ω, respectively. Since all HOCs were fabricated from the same wafer, thus their AMP is relatively same value.

All HOCs were fabricated from the same wafer, thus their read/write ability are relatively similar. However, a slightly offset may come from slider process.

Table 4.1 shows summary of electrical parameter of each HOC thickness before burnishing.

Table 4.1 Results of electrical measurement before burnishing

Parameters	HOC Thickness (Å)		
	24	20	16
Power to Contact (mW)	79.74 ± 5.00	82.52 ± 5.80	85.14 ± 3.96
Clearance (nm)	10.42 ± 0.66	10.51 ± 0.78	10.69 ± 0.54
Bit Error Rate (dcd)	-2.23 ± 0.24	-2.25 ± 0.28	-2.13 ± 0.17
Overwrite (dB)	-36.29 ± 3.35	-36.35 ± 3.23	-35.08 ± 1.46
Amplitude (μV)	13,415 ± 3509	16,185 ± 4801	13,727 ± 3711
Reader Resistance (Ω)	214.92 ± 26.85	248.18± 39.96	266.28 ± 39.16

After electrical measurement, head was treated by burnishing process. Head was moved to dwell for burnishing at the designated interference. The data of electrical measurement after burnishing were compared with reference data before burnishing to calculate degradation of each electrical parameter.

Table 4.2 shows the result of bit error rate and **Figure.4.1** shows delta of bit error rate (BER) of each HOC thickness at various interference levels compared to reference data.

Table 4.2 Results of bit error rate at each interference level

Interference Level (nm)	Bit Error Rate (decade)					
	HOC 16 Å		HOC 20 Å		HOC 24 Å	
	Actual	Delta	Actual	Delta	Actual	Delta
-4	-1.92	0.22	-1.77	0.52	-1.76	0.47
-3.5	-1.98	0.16	-1.83	0.41	-1.92	0.32
-3	-2.01	0.12	-1.96	0.32	-2.01	0.21
-2.5	-2.03	0.07	-1.94	0.31	-2.10	0.15
-2	-2.08	0.02	-2.05	0.22	-2.12	0.12
-1.5	-2.10	0.00	-2.13	0.18	-2.19	0.03
-1	-2.12	0.00	-2.17	0.10	-2.20	0.01
-0.5	-2.15	-0.02	-2.21	0.02	-2.22	0.00
0	-2.13	0.00	-2.23	0.00	-2.21	0.00
0.5	-2.14	0.00	-2.24	-0.01	-2.21	0.01
1	-2.14	0.00	-2.24	-0.01	-2.21	0.00

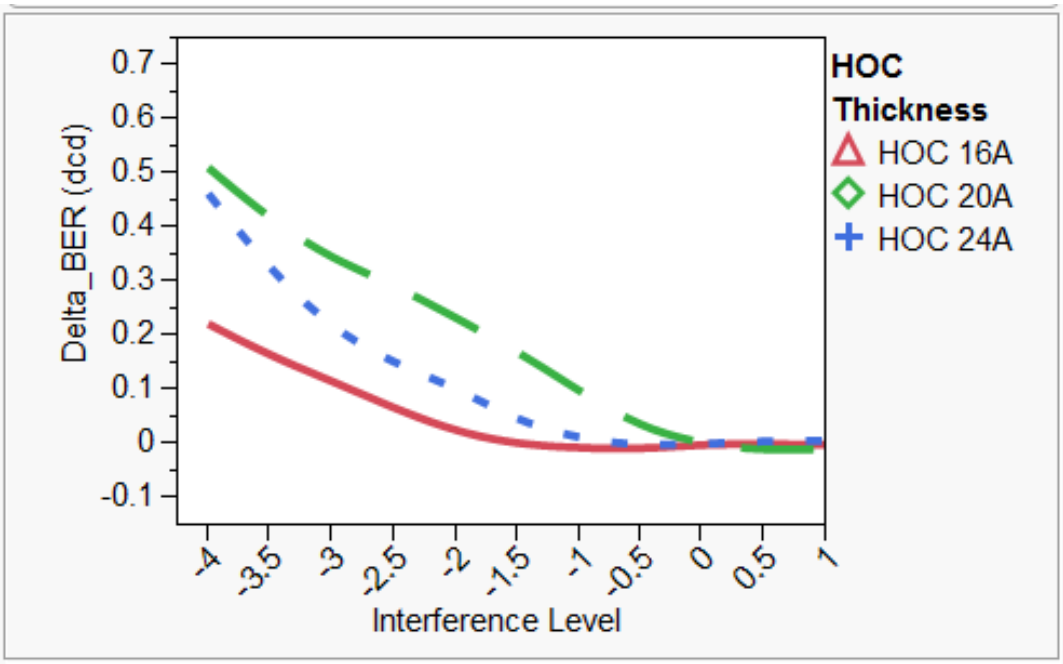

Figure 4.1 Degradation results of bit error rate

From **Figure 4.1**, at plus interference level, namely 0 to 1 level, delta BER of all HOC thickness was nearly zero. When the interference level increased to minus

level, the delta BER increased. At the -4 interference level, delta BERs of HOC 16, 20 and 24 Å were 0.22, 0.52 and 0.47 decade, respectively.

HOC 16 Å shows the lowest degradation while HOCs 20 Å and 24 Å show relatively high degradation. HOCs 20 and 24 Å have the same adhesion layer (type B) and thickness but difference in DLC thickness and quality (types C and D, respectively). HOCs 16 Å and 20 Å were coated with the same quality and thickness of DLC (type C) but different thickness and type of adhesion layer (types A and B, respectively). HOC 16 Å based on adhesion layer (type A) with a thinner thickness of adhesion layer provides a strong bonding between DLC and magnetic layer surface, resulting in a slow degradation. Form above results, type of adhesion layer is a key for slow degradation.

Table 4.3 shows the result of overwrite and **Figure 4.2** shows delta of overwrite (OVW) of each HOC thickness at various interference levels compared to reference data to confirm write ability.

Table 4.3 Results of overwrite at each interference level

Interference Level (nm)	Overwrite (dB)					
	HOC 16 Å		HOC 20 Å		HOC 24 Å	
	Actual	Delta	Actual	Delta	Actual	Delta
-4	-32.55	2.70	-31.17	5.71	-31.92	4.66
-3.5	-33.36	1.83	-31.14	5.13	-33.68	2.90
-3	-33.61	1.52	-32.04	4.62	-34.04	2.26
-2.5	-34.22	0.88	-32.28	3.67	-35.01	1.84
-2	-34.92	0.18	-33.70	2.90	-34.99	1.71
-1.5	-34.92	0.22	-34.39	2.56	-36.47	0.08
-1	-34.95	0.13	-35.15	1.24	-36.25	0.03
-0.5	-35.36	-0.28	-35.94	0.22	-36.22	0.06
0	-35.10	-0.01	-36.52	-0.16	-36.37	-0.09
0.5	-35.14	-0.06	-36.78	-0.42	-36.49	-0.21
1	-35.20	-0.12	-36.36	0.00	-36.15	0.13

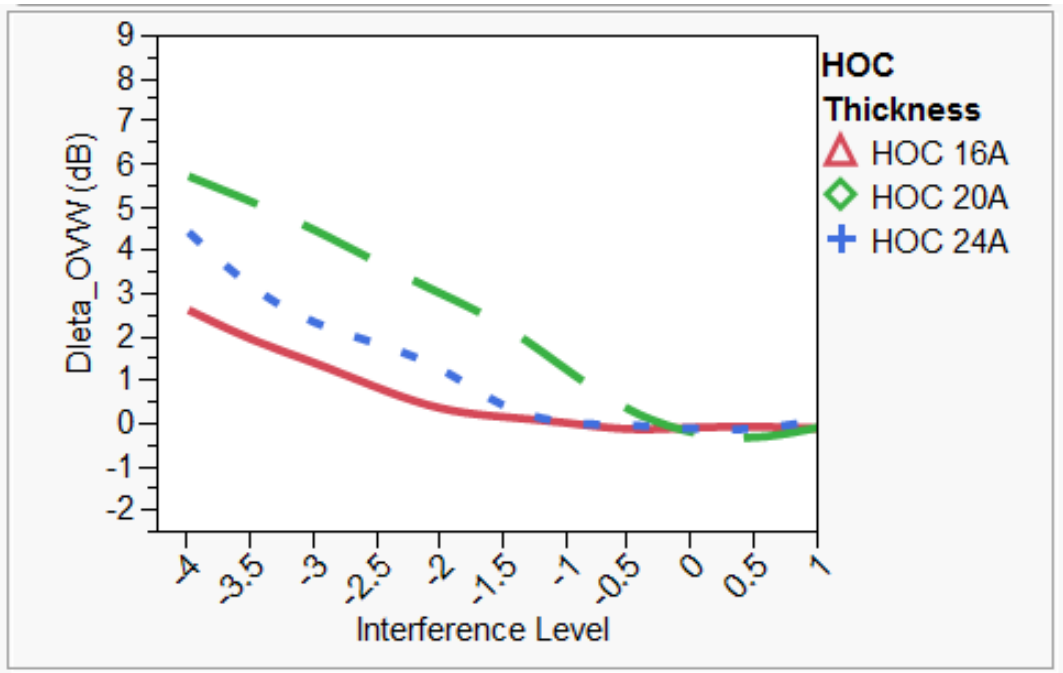

Figure 4.2 Degradation results of overwrite

From **Figure 4.2**, at plus interference level, namely 0 to 1 level, delta OVW of all HOC thicknesses was nearly zero. When the interference level increased to minus

level, the delta OVW increased. At the -4 interference level, delta OVWs of HOC 16, 20 and 24 Å were 2.70, 5.71 and 4.66 dB, respectively.

Similarly to BER properties, HOC 16 Å shows the lowest degradation while HOCs 20 Å and 24 Å show relatively high degradation. HOCs 20 and 24 Å have the same adhesion layer (type B) and thickness but difference in DLC thickness and quality (types C and D, respectively). HOCs 16 Å and 20 Å were coated with the same quality and thickness of DLC (type C) but different thickness and type of adhesion layer (types A and B, respectively). HOC 16 Å based on adhesion layer (type A) with a thinner thickness of adhesion layer provides a strong bonding between DLC and magnetic layer surface, resulting in a slow degradation. Form above results, type of adhesion layer is a key for slow degradation.

Table 4.4 shows the result of amplitude and **Figure 4.3** shows delta of amplitude (AMP) of each HOC thickness at various interference levels compared to reference data to confirm read ability.

Table 4.4 Results of amplitude at each interference level

Interference Level (nm)	Amplitude					
	HOC 16 Å		HOC 20 Å		HOC 24 Å	
	Actual (μV)	Delta (%)	Actual (μV)	Delta (%)	Actual (μV)	Delta (%)
-4	13684.61	-3.48	15603.92	-12.88	11786.48	-15.23
-3.5	14008.22	1.15	16172.19	-7.66	12462.43	-11.07
-3	14244.09	2.25	16717.46	-4.69	13499.48	-5.10
-2.5	14330.82	1.27	15549.34	-3.88	13586.86	-3.32
-2	14405.47	1.71	16522.21	-1.25	13414.72	-1.42
-1.5	14351.43	1.12	17245.67	0.15	13651.35	0.33
-1	13993.60	1.12	17137.75	0.17	13715.26	0.35
-0.5	13769.04	0.29	16628.74	0.04	13661.37	-0.11
0	13690.79	-0.35	16189.98	0.02	13571.53	-0.73
0.5	13654.30	-0.69	16164.32	-0.14	13502.60	-1.31
1	13649.48	-0.64	16130.88	-0.37	13637.21	-0.32

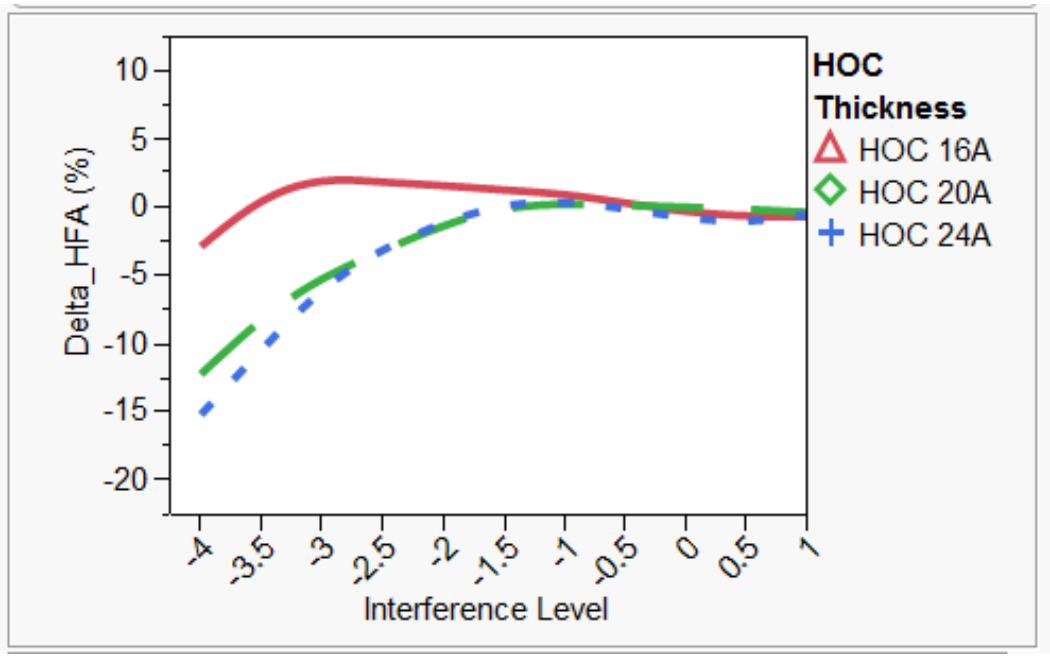

Figure 4.3 Degradation results of amplitude

From **Figure 4.3**, at plus interference level, namely 0 to 1 level, delta AMP of all HOC thicknesses was nearly zero. When the interference level increased to minus level, the delta AMP decreased. At the -4 interference level, delta AMPs of HOC 16, 20 and 24 Å were -3.48, -12.88 and -15.23%, respectively.

Similarly to BER properties, HOC 16 Å shows the lowest degradation in amplitude while HOCs 20 Å and 24 Å show relatively high degradation in amplitude. HOCs 20 and 24 Å have the same adhesion layer (type B) and thickness but difference in DLC thickness and quality (types C and D, respectively). HOCs 16 Å and 20 Å were coated with the same quality and thickness of DLC (type C) but different thickness and type of adhesion layer (types A and B, respectively). HOC 16 Å based on adhesion layer (type A) with a thinner thickness of adhesion layer provides a strong bonding between DLC and magnetic layer surface, resulting in a slow degradation. Form above results, type of adhesion layer is a key for slow degradation.

Table 4.5 shows the result of reader resistance and **Figure 4.4** shows delta of reader resistance (RD_RES) of each HOC thickness at various interference levels compared to reference data to confirm head burnishing.

Table 4.5 Results of reader resistance at each interference level

Interference Level (nm)	Reader Resistance					
	HOC 16 Å		HOC 20 Å		HOC 24 Å	
	Actual (Ω)	Delta (%)	Actual (Ω)	Delta (%)	Actual (Ω)	Delta (%)
-4	282.00	2.38	274.27	3.08	237.29	8.78
-3.5	276.31	1.57	259.80	0.86	232.01	6.31
-3	275.69	1.47	256.99	-0.58	230.83	4.20
-2.5	276.83	0.29	246.20	0.25	225.51	1.98
-2	277.01	0.35	247.46	0.15	220.92	0.28
-1.5	275.61	0.42	254.51	-0.29	217.00	-0.34
-1	272.29	0.82	251.64	0.10	215.34	-0.09
-0.5	267.11	0.32	248.74	0.24	215.88	0.18
0	267.20	0.35	246.56	0.45	216.29	0.36
0.5	267.62	0.52	246.08	0.22	216.19	0.33
1	266.89	0.24	245.81	0.13	215.98	0.23

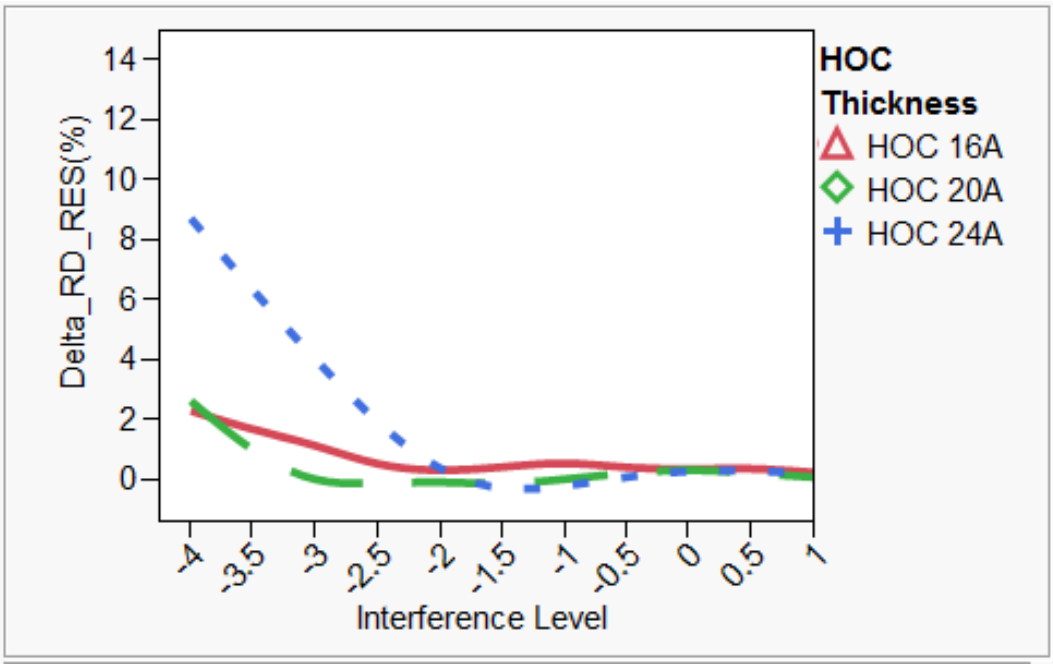

Figure 4.4 Degradation results of reader resistance

From **Figure 4.4**, at plus interference level, namely 0 to -0.5 levels, delta RD_RES of all HOC thicknesses was nearly zero. When the interference level increased above -0.5 level, the delta RD_RES increased. At the -4 interference level, delta RD_RES of HOC 16, 20 and 24 Å were 2.38, 3.08 and 8.78%, respectively.

HOC 16 Å and HOCs 20 Å show lower degradation while and 24 Å show higher degradation in RD_RES properties. HOCs 20 Å and 24 Å have the same adhesion layer type (type B) and thickness but difference in DLC thickness and quality. Adhesion layer type (type B) does not provide good bonding. DLC film is worn easily. After HOC was totally worn, reader will directly interact with media. The lower reader resistance is more sensitive for protrusion and easily to damage by mechanical interaction, resulted in significant change in reader resistance before and after burnishing (high delta RD_RES). Low reader resistance is cause for higher delta RD_RES of HOC 24 Å, while high reader resistance is effective for small degradation. Moreover, HOCs 16 Å and 20 Å were coated with the same quality and thickness of DLC but different thickness and type of adhesion layer (Materials A and B, respectively). HOC 16 Å based on adhesion layer (Material A) with a thinner thickness of adhesion layer provides a strong bonding between DLC and magnetic layer surface, resulting in an effective DLC film on magnetic layer protection, providing a lower degradation.
From above results, thinner adhesion layer and type of adhesion layer (type A) are key parameters for lower degradation.

Table 4.6 shows the result of clearance and **Figure 4.5** shows delta of clearance of each HOC thickness at various interference levels compared to reference data to confirm head burnishing.

Table 4.6 Results of clearance at each interference level

Interference Level (nm)	Clearance (nm)					
	HOC 16 Å		HOC 20 Å		HOC 24 Å	
	Actual	Delta	Actual	Delta	Actual	Delta
-4	12.25	1.72	12.74	2.28	13.35	3.08
-3.5	12.03	1.50	12.61	2.15	12.98	2.71
-3	11.92	1.39	12.27	1.81	12.55	2.28
-2.5	11.71	1.19	11.89	1.44	12.14	1.87
-2	11.63	1.11	11.57	1.11	11.61	1.33
-1.5	11.40	0.88	11.26	0.81	11.16	0.89
-1	11.23	0.71	11.02	0.56	10.75	0.48
-0.5	10.99	0.47	10.75	0.30	10.51	0.23
0	10.59	0.07	10.46	0.00	10.24	-0.03
0.5	10.52	-0.01	10.45	0.00	10.20	-0.07
1	10.53	0.01	10.45	0.00	10.26	-0.01

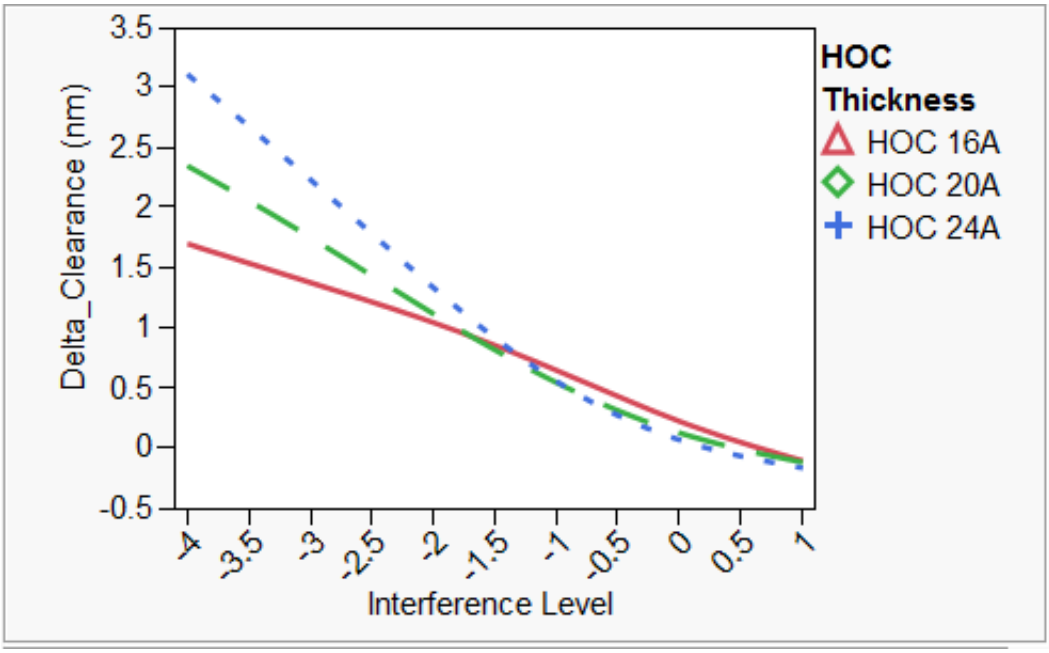

Figure 4.5 Degradation results of clearance

From Figure 4.5, at plus interference level, namely 0 to 1 levels, delta clearance of all HOC thicknesses was zero. When the interference level increased to

minus level, the delta clearance increased. At the -4 interference level, delta clearance of HOC 16, 20 and 24 Å were 1.72, 2.28 and 3.08 nm, respectively.

HOCs 20 Å and 24 Å have the same adhesion layer type (type B) and thickness but difference in DLC thickness and quality. Adhesion layer type (type B) does not provide good bonding. DLC film is worn easily. After HOC was totally worn, reader will directly interact with media. Low reader resistance is more sensitive for protrusion. Reader might be severely damaged during mechanical interaction. Low reader resistance is a cause for higher delta clearance of HOC 24 Å. Moreover, HOCs 16 Å and 20 Å were coated with the same quality and thickness of DLC but different thickness and type of adhesion layer. HOC 16 Å based on adhesion layer (type A) with a thinner thickness of adhesion layer provides a strong bonding between DLC and magnetic layer surface, resulting in an effective DLC film on magnetic layer protection, providing a small degradation.

Table 4.7 shows the result of power to contact and **Figure 4.6** shows delta of power to contact (PtC) of each HOC thickness at various interference levels compared to reference data to confirm relationship with clearance.

Table 4.7 Results of power to contact at each interference level

Interference Level (nm)	Power to Contact (mW)					
	HOC 16 Å		HOC 20 Å		HOC 24 Å	
	Actual	Delta	Actual	Delta	Actual	Delta
-4	98.01	14.48	99.85	17.82	101.33	22.97
-3.5	96.39	12.86	99.01	16.98	98.56	20.19
-3	95.15	11.61	96.33	14.30	95.09	16.72
-2.5	93.31	9.78	93.32	11.29	92.85	14.48
-2	92.74	9.20	91.04	9.01	88.72	10.35
-1.5	91.10	7.57	88.26	6.24	85.71	7.34
-1	89.48	5.95	86.45	4.42	82.45	4.09
-0.5	87.76	4.22	84.15	2.12	80.42	2.05
0	84.36	0.82	81.80	-0.23	77.98	-0.39
0.5	83.63	0.09	81.75	-0.28	77.78	-0.59
1	83.62	0.08	81.55	-0.48	78.16	-0.20

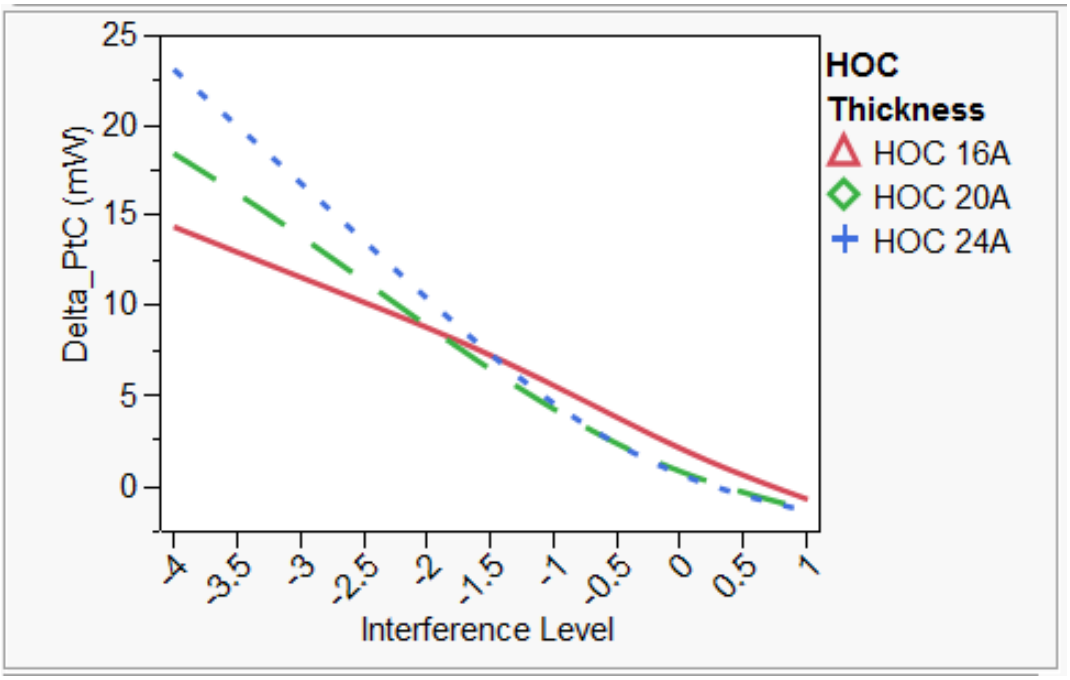

Figure 4.6 Degradation results of power to contact

From **Figure 4.6**, at plus interference level, namely 0 to 1 levels, delta PtC of all HOC thicknesses was nearly zero. When the interference level increased to minus

level, the delta clearance increased. At the -4 interference level, delta clearance of HOC 16, 20 and 24 Å were 14.48, 17.82 and 22.97 mW, respectively. This parameters used for confirm relationship with clearance which all HOC thicknesses show reasonable relationship between clearance and power to contact.

Table 4.8 shows delta of each electrical parameters at final interference level (-4nm) of each HOC thickness.

Table 4.8 Delta electrical parameters at final interference level

Delta electrical parameters	HOC 16 Å	HOC 20 Å	HOC 24 Å
Bit error rate (dcd)	0.22	0.52	0.47
Overwrite (dB)	2.70	5.71	4.66
Amplitude (%)	-3.48	-12.88	-15.23
Reader Resistance (%)	2.38	3.08	8.78
Clearance (nm)	1.72	2.28	3.08
Power to contact (mW)	14.48	17.82	22.97

The results of read/write performance characterization of three types of HOCs can summarize as follows;

(1) Adhesion layer type significantly effects on read/write performance and wear behaviors. Compare between HOCs 16 and 20 Å, which was used difference adhesion layer type, the HOC 16 Å shows small degradation. This may due to adhesion layer type A provide good bonding to DLC layer. Then, DLC is not easily worn away. Head is effectively protected by DLC during burnishing when interference level increasing.

(2) Thickness of HOC has a minor effect on read/write behaviors. In the case of HOCs 20 and 24 Å, which have different DLC thickness and density with the same adhesion layer thickness, the HOC 20 Å shows slightly fast degradation than HOC 24 Å.

From the read/write performance characterization results, HOC 16 Å shows the best condition for read/write performance.

4.3 Effect of HOC thickness on head topography

Wear may occur on the slider surface during read/write process at electrical measurement. To confirm wear, burnished area of head was characterized by AFM under condition explained in 3.2.3. Figure 4.7 shows 3D-AFM image of head after burnishing representing writer (a) and reader (b) areas around pole tip.

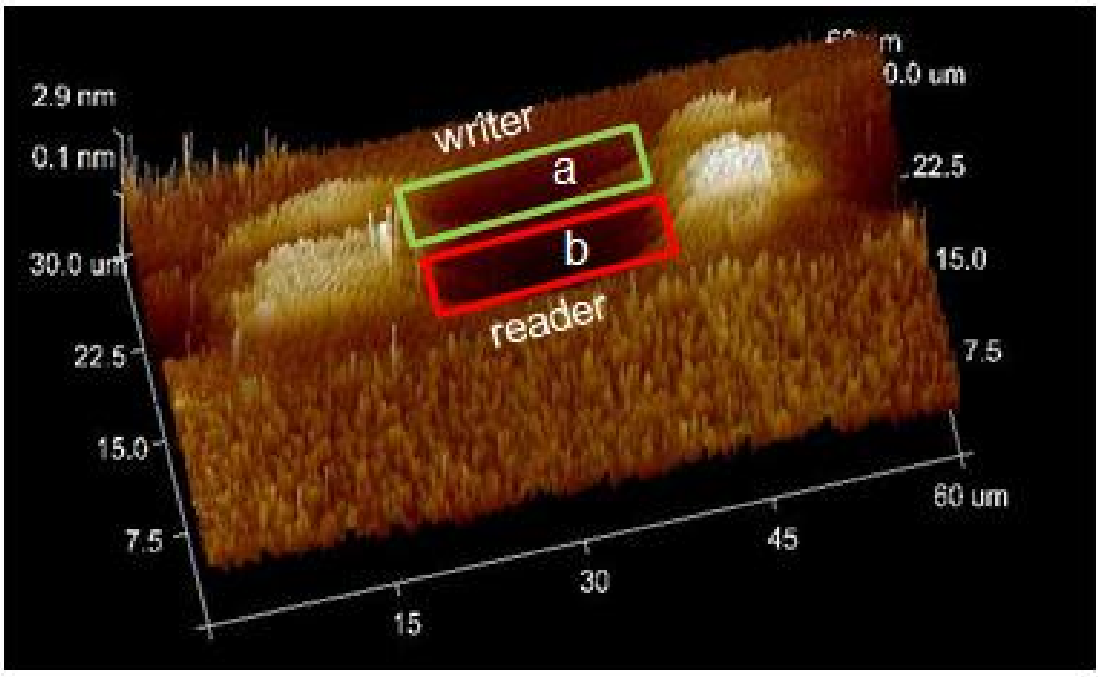

Figure 4.7 3D-AFM image of head after burnishing

Figure 4.8 shows AFM image of HOC 16 Å and its wear depth data were summarized in **Table 4.3**

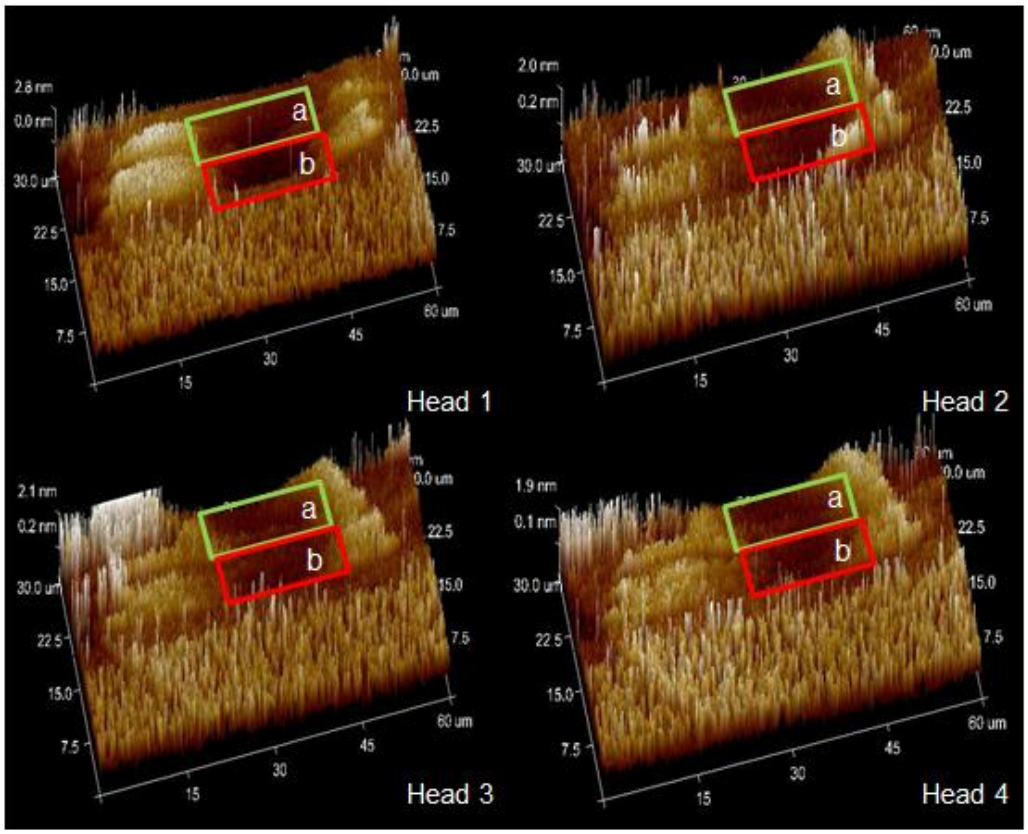

Figure 4.8 3D- AFM image of HOC 16 Å after burnishing

Table 4.3 Summary of wear depth of HOC 16 Å

Head Number	Wear depth at writer area (nm)	Wear depth at reader area (nm)
1	2.196	2.604
2	1.446	1.470
3	1.396	1.366
4	1.326	1.347
Average	1.591±0.406	1.697±0.607

AFM images of all heads show wear depth in write and reader areas as a dark color. Wear depth of writer (area a) of heads 1, 2, 3 and 4 were 2.196, 1.446, 1.396 and 1.326 nm, respectively, while that of reader (area b) of 1, 2, 3 and 4 were 2.604, 1.470, 1.366 and 1.347 nm, respectively. The average wear depth of writer and reader is 1.591±0.406 and 1.697±0.607 nm, respectively.

Head 1 shows the deepest wear depths of both writer and reader. HOC is likely worn away before final interference level. Reader and writer were damaged directly by mechanical interaction between head and disk.

Heads 2, 3 and 4 shows a shallower wear depth in write and reader areas. Heads are not totally damaged by mechanical interaction between head and disk. HOC should provide protection to head until final interference level.

From wear depth results, HOC **16** Å can act as an effective HOC to protect head from head-disk interaction until final interference level. Head is not totally directly interacted with disk then less head damage and less wear depth.

Figure 4.9 shows AFM image of HOC 20 Å and its wear depth data were summarized in **Table 4.4**

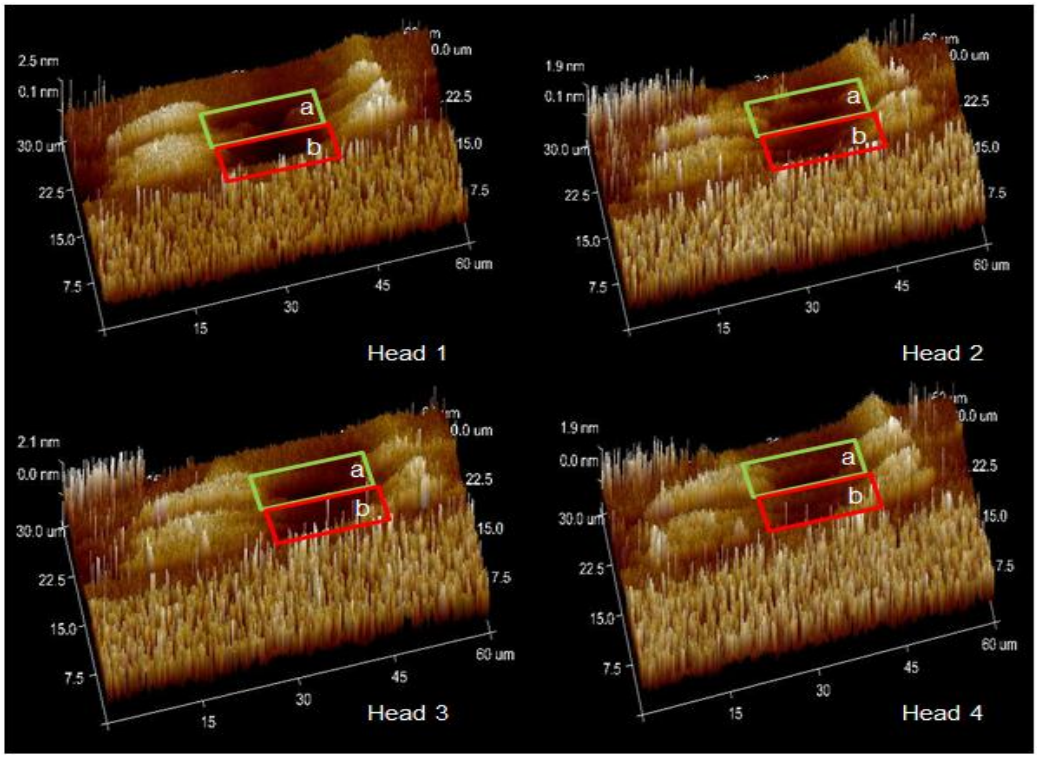

Figure 4.9 3D- AFM image of HOC 20 Å after burnishing

Table 4.4 Summary of wear depth of HOC 20 Å

Head Number	Wear depth at writer area (nm)	Wear depth at reader area (nm)
1	2.330	2.777
2	1.817	1.622
3	1.886	1.418
4	2.332	1.386
Average	2.091±0.278	1.801±0.659

AFM images of all heads show wear depth in write and reader areas as a dark color. Wear depth of writer (area a) of heads 1, 2, 3 and 4 were 2.330, 1.817, 1.886 and 2.332 nm, respectively, while that of reader (area b) of 1, 2, 3 and 4 were 2.777, 1.622, 1.418 and 1.386 nm, respectively. The average wear depth of writer and reader is 2.091±0.278 and 1.801±0.659 nm, respectively. The average of wear depth of writer and reader of HOC 20 Å is higher than that of HOC 16 Å, showing higher severe level of wear. HOC is likely worn away before final interference level. Reader and writer were damaged directly by mechanical interaction between head and disk especially writer area.

From wear depth results, HOC 20 Å cannot act as effective HOC to protect head from head-disk interaction until final interference level. After HOC totally worn away, head is directly interacted with disk, resulting in significant wear damage on writer and reader.

Figure 4.10 shows AFM image of HOC 24 Å and its wear depth data were summarized in **Table 4.5**

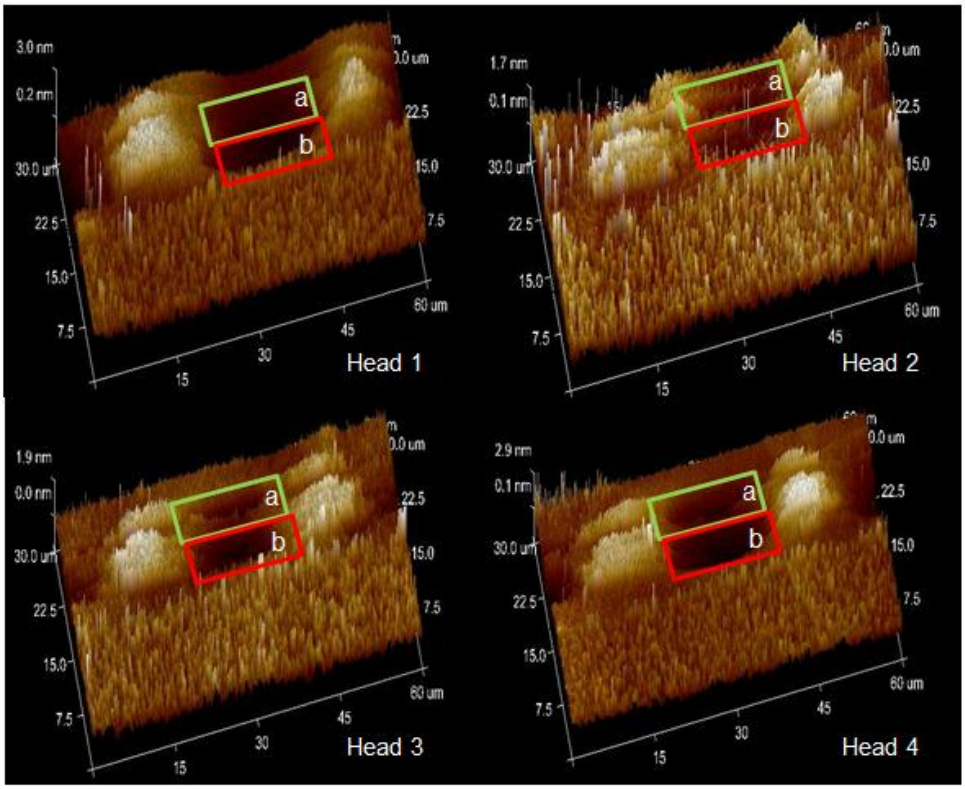

Figure 4.10 3D- AFM image of HOC 24 Å after burnishing

Table 4.5 Summary of wear depth of HOC 24 Å

Head Number	Wear depth at writer area (nm)	Wear depth at reader area (nm)
1	2.240	2.757
2	1.324	1.778
3	1.388	2.727
4	2.408	3.617
Average	1.840±0.564	2.720±0.751

AFM images of all heads show wear depth in write and reader areas as a dark color. Wear depth of writer (area a) of heads 1, 2, 3 and 4 were 2.240, 1.324, 1.388 and 2.408 nm, respectively, while that of reader (area b) of 1, 2, 3 and 4 were 2.757, 1.778, 2.727 and 3.617 nm, respectively. The average wear depth of writer and reader is 1.840±0.564 and 2.720±0.751 nm, respectively. The average of wear depth of writer and reader of HOC 24 Å is higher than that of HOC 16 Å but relatively comparable to that 20 Å, showing higher severe level of wear. HOC is likely worn away before final

interference level. Reader and writer were damaged directly by mechanical interaction between head and disk especially writer area.

From wear depth results, HOC 24 Å cannot act as effective HOC to protect head from head-disk interaction until final interference level. After HOC totally worn away, head is directly mechanically interacted with disk, resulting in significant wear damage on writer and reader.

Table 4.6 shows the summary result of wear depth of all HOC thickness.

Table 4.6 Summary of wear depth at writer and reader area of each HOC thickness

HOC Thickness	Wear depth at writer area (nm)	Wear depth at reader area (nm)
16 Å	1.591±0.406	1.697±0.607
20 Å	2.091±0.278	1.801±0.659
24 Å	1.840±0.564	2.720±0.751

The results of topography characterization of three types of HOCs can summarize as follows;

(1) HOC 16 Å (adhesion layer type A and DLC type C) shows the shallowest wear depth, implying the smallest head damage. HOCs 20 (adhesion layer type B and DLC type C) and 24 Å (adhesion layer type B and DLC type D) shows deeper wear depth than HOC 16 Å, implying significant head damage.

(2) Adhesion layer type effects on topography behaviors. Difference adhesion material shows difference bonding properties between DLC and magnetic layer. In the case of HOCs 16 and 20 Å, their adhesion layer materials are different but DLC layers are the same. HOC 16 Å shows less wear depth. This may due to adhesion layer type A provides good bonding to DLC layer. Then, DLC is not easily worn away until final interference level (-4 nm). Head was protected during burnishing, thus a shallower wear depth in HOC 16 Å of HGA. Adhesion material A shows superior adhesive property than adhesive material B.

From the topography characterization results, HOC 16 Å shows the best condition against wear depth.

4.4 Effect of HOC thickness on wear resistance

After electrical measurement and AFM measurement, head was characterized by SEM to investigate wear resistance, contamination and position of wear by condition described in 3.2.4.

Figure 4.11 shows FESEM Image of head before burnishing, representing writer and reader areas around pole tip.

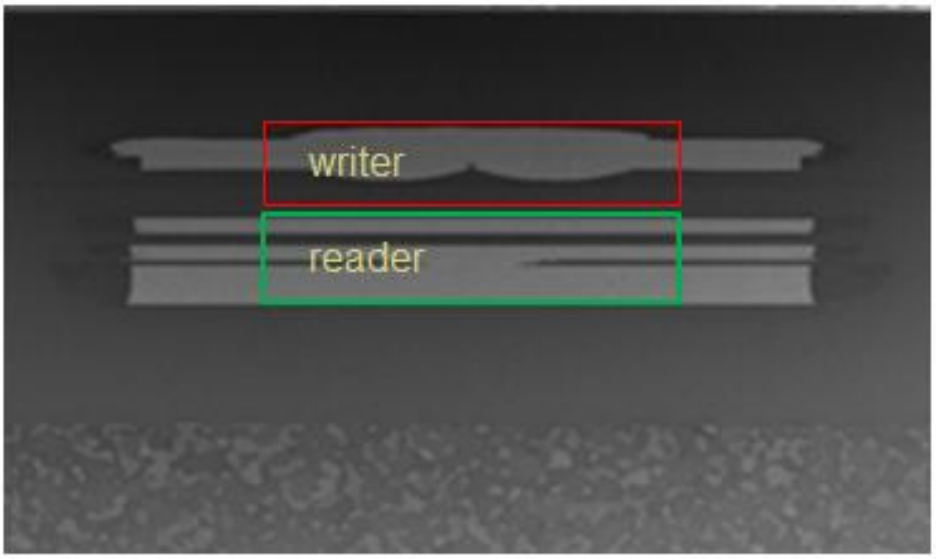

Figure 4.11 FESEM Image of head before burnishing

Figure 4.12 shows FESEM images of 4 heads of HOC 16 Å.

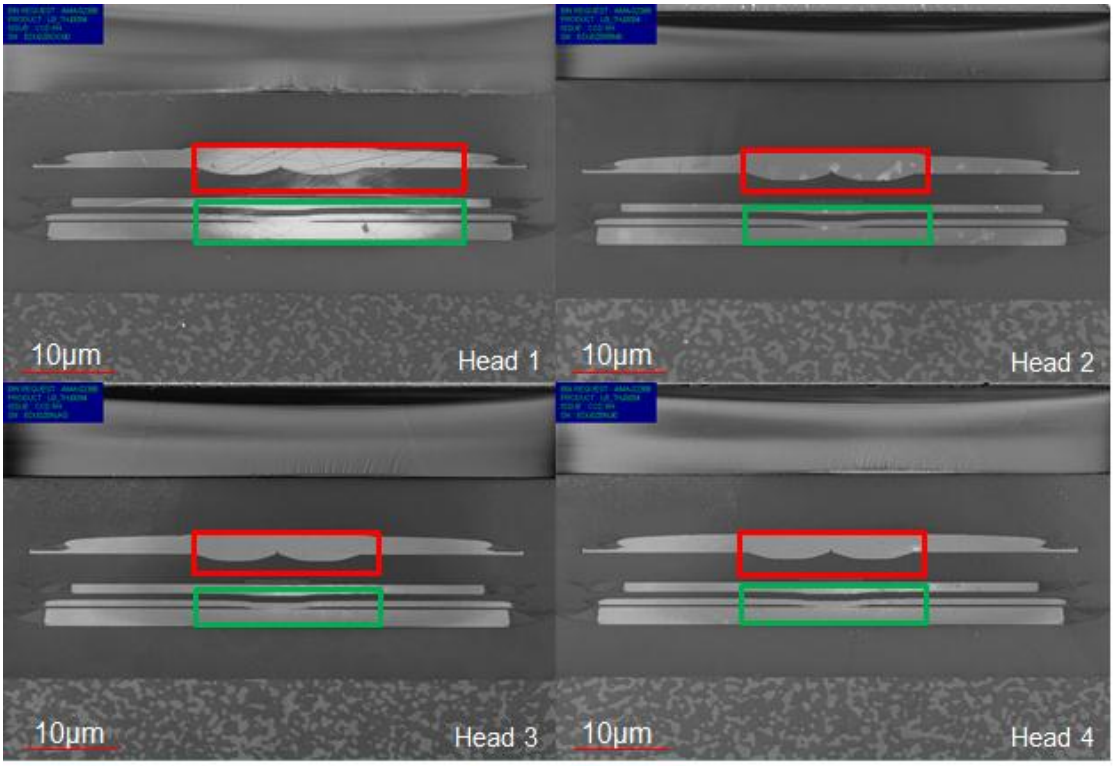

Figure 4.12 FESEM Images of head with HOC 16 Å

Compare to head before burnishing, there are bright contrast appeared on writer and reader areas after burnishing. This bright contrast was determined as wear. To compare the occurred wear of each HOC thickness, the wear area was calculated.

Head 1 shows the brightest contrast on writer and reader areas, implying a severe wear especially at reader area. This result is coincided with AFM image and electrical measurement. The wear areas at write and reader are 78.45 and 113.92 μm^2, respectively.

Head 2 shows the less bright contrast on both writer and reader areas, implying a less severe wear. This result is coincided with AFM image and electrical measurement.

Heads 3 and 4 show similar wears behavior. Slightly bright contrast was found in only reader area, implying a wear on reader while less wear on writer. The wear area at reader of heads 3 and 4 are 48.54 and 45.60 μm^2, respectively. Due to its small wear area, the occurred wear is considered as not significant wear. These results are coincided with AFM images and electrical measurement.

From above results, HOC 16 Å shows non-significant wear on pole tip. Head should be protected by HOC until final interference level of electrical measurement.

The wear area of each head of HOC 16 Å is summarized in **Table 4.1**

Table 4.1 Wear area at writer and reader areas of HOC 16 Å

Head number	Wear at writer area (μm^2)	Wear at reader area (μm^2)
1	78.45	113.92
2	0	0
3	0	48.54
4	0	45.60
Average	19.61±39.22	52.01±46.87

Figure 4.13 shows FESEM images of 4 heads of HOC 20 Å

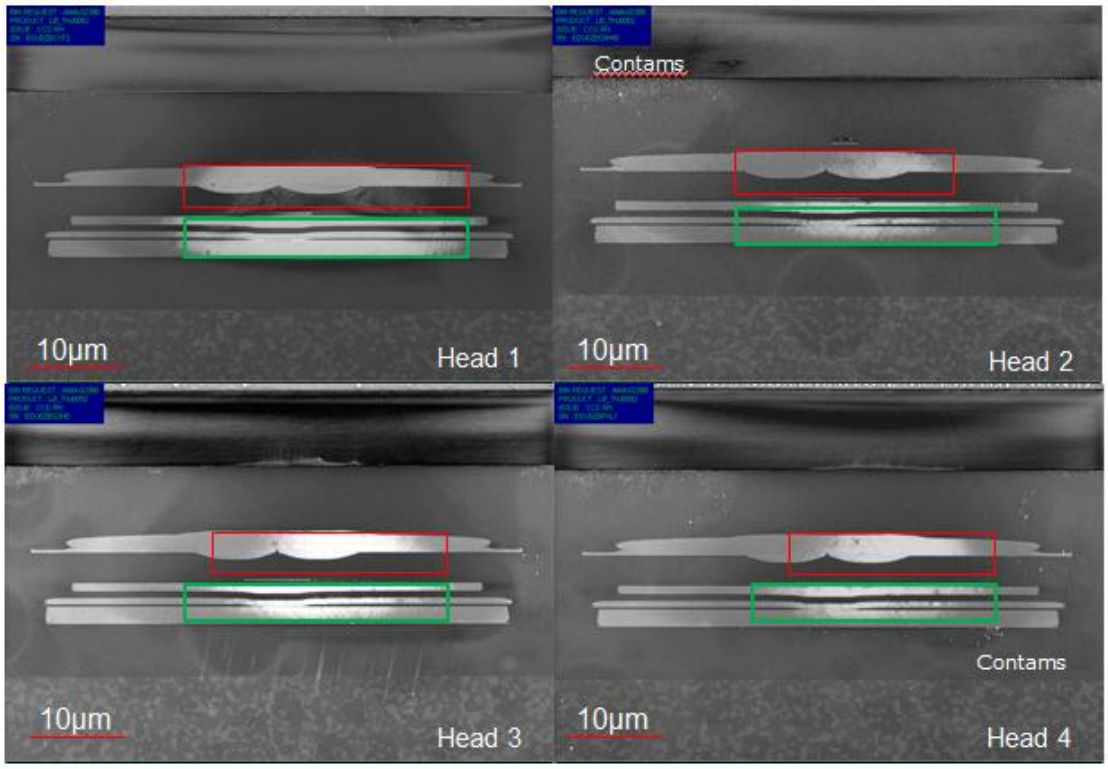

Figure 4.13 FESEM Images of head with HOC 20 Å

Heads 1, 2, 3 and 4 show the significant bright contrast on writer and reader areas, implying a severe wear. This result is coincided with AFM image and electrical measurement. The wear at writer area is 76.14, 35.09, 55.30 and 42.76μm^2, respectively while reader area is 128.20, 78.41, 84.32 and 76.52 μm^2, respectively.

From above results, HOC 20 Å shows significant wear on pole tip. Head should not be protected by HOC until final interference level of electrical measurement.

The wear area of each head of HOC 20 Å is summarized in **Table 4.2**

Table 4.2 Wear area at writer and reader areas of HOC 20 Å

Head number	Wear at writer area (μm^2)	Wear at reader area (μm^2)
1	76.14	128.20
2	35.09	78.41
3	55.30	84.32
4	42.76	76.52
Average	52.32±17.93	91.86±24.45

Figure 4.14 shows FESEM images of 4 heads of HOC 24 Å

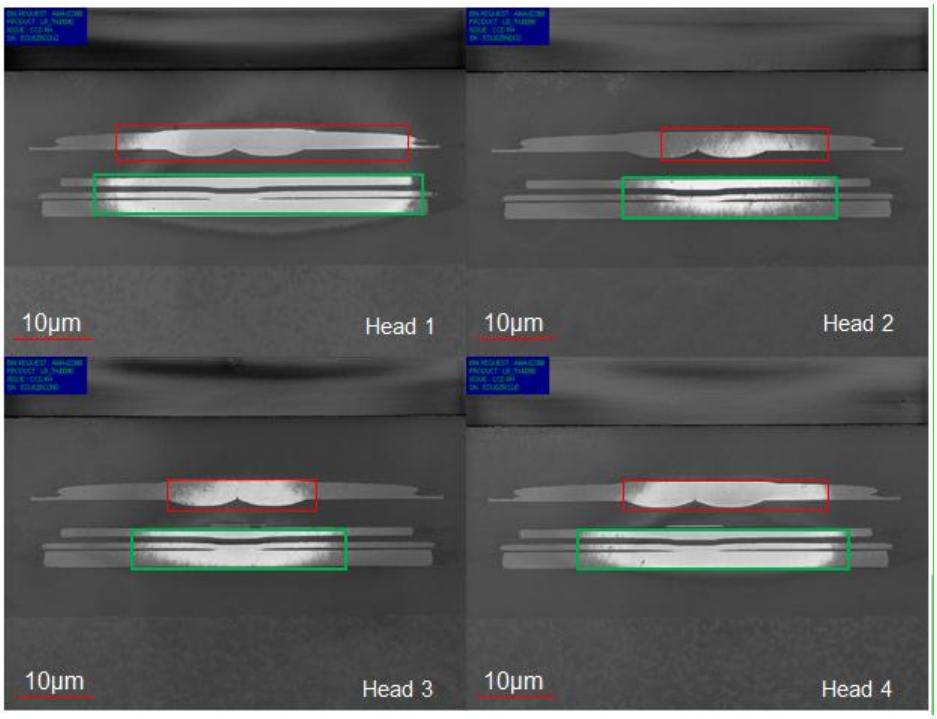

Figure 4.14 FESEM Images of head with HOC 24 Å

Heads 1, 2, 3 and 4 show the significant bright contrast on writer and reader areas, implying a severe wear. This result is coincided with AFM image and electrical measurement. The wear at writer area is 111.08, 36.80, 46.08 and 62.14 μm^2, respectively while reader area is 144.84, 79.97, 105.04 and 122.10 μm^2, respectively.

From above results, HOC 24 Å shows significant wear on pole tip. Head should not be protected by HOC until final interference level of electrical measurement.

The wear area of each head of HOC 24 Å is summarized in **Table 4.3**

Table 4.3 Wear area at writer and reader areas of HOC 24 Å

Head number	Wear at writer area (μm^2)	Wear at reader area (μm^2)
1	111.08	144.84
2	36.80	79.97
3	46.08	105.04
4	62.14	122.20
Average	64.02±33.07	113.01±27.40

Table 4.4 shows the summary result of wear area of all HOC thickness.

Table 4.4 Summary of wear area at writer and reader area of each HOC thickness

HOC Thickness	Wear at writer area (μm^2)	Wear at reader area (μm^2)
16 Å	19.61±39.22	52.01±46.87
20 Å	52.32±17.93	91.86±24.45
24 Å	64.02±33.07	113.01±27.40

The results of wear resistance characterization of three types of HOCs can summarize as follows;

(1) HOC 16 Å (adhesion layer type A and DLC type C) shows the smallest wear area, implying the smallest head damage. HOCs 20 (adhesion layer type B and DLC type C) and 24 Å (adhesion layer type B and DLC type D) shows larger wear area than HOC 20 Å, implying significant head damage.

(2) Adhesion layer type effects on wear behaviors. Difference adhesion material shows difference bonding properties between DLC and magnetic layer. In the case of HOCs 16 and 20 Å, their adhesion layer materials are different but DLC layers are the same. HOC 16 Å shows smaller wear area. This may due to adhesion layer type A provides good bonding to DLC layer. Then, DLC is not easily worn away until final interference level (-4 nm). Head was protected during burnishing, thus a smaller wear area in HOC 16 Å of HGA. Adhesion material A shows superior adhesive property than adhesive material B.

From the wear resistance characterization results, HOC 16 Å shows the optimum condition for wear resistance.

CHAPTER 5
CONCLUSIONS AND SUGGESTION

5.1 Conclusions

In this thesis, effect of head overcoat (HOC) thickness of head gimbal assembly (HGA) for head media spacing (HMS) reduction was investigated. Three types of HOC thickness were used in this study; HOC 16, 20 and 24 Å. HOC consists of diamond-like carbon (DLC) layer and adhesion layer for bonding DLC and magnetic layer. The details of each HOC thickness are shown as follows;

HOC 16 Å consists of adhesion layer type A and DLC layer type C.
HOC 20 Å consists of adhesion layer type B and DLC layer type C.
HOC 24 Å consists of adhesion layer type B and DLC layer type D.

Thickness of adhesion layer of type A is thinner than that of type B and thickness of DLC layer of type C is thinner than that of type D. The reliability of all HOC thicknesses was characterized in terms corrosion, read/write performance and wear.

The summary of reliability test results is as follows;

(i) Corrosion behavior: After HAST, all HOCs show a number of corrosion positions in an acceptable range. This result implies that the adhesion layer types A and B, and DLC layer types C and D at the thickness range in this study is effective protection against corrosion.

(ii) Read/write performance: Electrical measurement before and after burnishing at interference level +1 to -4 nm was measured on spin-stand tester in terms of power to contact (PtC), clearance, bit error rate (BER), overwrite (OVW), amplitude (AMP) and reader resistance (RD_RES). The delta of each electrical parameter before and after burnishing was prepared to determine its reliability.

- HOC 16 Å shows the smallest delta of electrical parameters at final interference level (-4 nm). Delta of BER, OVW, AMP and RD_RES is 0.22 decade, 2.70 dB, -3.84% and 2.38%, respectively.

- HOC 20 Å shows delta of BER, OVW, AMP and RD_RES as 0.52 decade, 5.71 dB, -12.88% and 3.08%, respectively, at final interference level (-4 nm).

- HOC 24 Å shows delta of BER, OVW, AMP and RD_RES as 0.47 decade, 4.66 dB, 15.23% and 8.78%, respectively, at final interference level (-4 nm.

This result shows that HOC 16 Å has the best robustness for read/write performance, while HOCs 20 and 24 Å show the large delta of electrical parameters, implying degradation in read/write performance. HOCs 20 and 24 Å could not provide good protection until the final interference level.

(iii) Wear topography behavior: Topography of wear depth of HGA after read/write performance characterization was measured by atomic force microscopy (AFM).

-HOC 16 Å shows non-significant wear depth on both writer and reader area. Wear depth at writer and reader area is 1.6 and 1.7 nm, respectively.

-HOC 20 Å shows significant wear depth on both writer and reader area. Wear depth at writer and reader area is 2.0 and 1.8 nm, respectively.

-HOC 24 Å shows significant wear depth on both writer and reader area. Wear depth at writer and reader area is 1.8 and 2.7 nm, respectively.

This result shows that HOC 16 Å has the best protection for transducer while HOCs 20 and 24 Å could not protect transducer till final interference level.

(iv) Wear resistance behavior: After topography characterization, wear resistance was characterized by field emission scanning electron microscopy (FESEM) and its wear area was calculated.

-HOC 16 Å shows non-significant wear. Wear area of writer and reader is 22 and 54 μm^2, respectively.

-HOC 20 Å shows significant wear. Wear area of writer and reader is 52 and 92 μm^2, respectively.

-HOC 24 Å shows significant of wear. Wear area of writer and reader is 64 and 113 μm^2, respectively.

This result shows that HOC 16 Å has the best protection for transducer while HOCs 20 and 24 Å could not protect untill final interference level.

The summary result of all reliability characterization is shown in **Table 5.1**

Table 5.1 Summary result of characterization types

Reliability properties	**Thickness**		
	HOC 16 Å	**HOC 20 Å**	**HOC 24 Å**
1. Corrosion	Acceptable	Acceptable	Acceptable
2. Read/write performance			
-Delta Bit error rate (dcd)	0.22	0.52	0.47
-Delta Overwrite (dB)	2.70	5.71	4.66
-Delta Amplitude (%)	-3.84	-12.88	-15.23
-Delta Reader resistance (%)	2.38	3.08	8.78
-Delta Clearance (nm)	1.72	2.38	3.08
-Delta Power to contact (mW)	14.48	17.82	22.97
3. Wear depth (nm)			
- Writer Area	1.6	2.0	1.8
- Reader Area	1.7	1.8	2.7
4. Wear area (μm)			
- Writer Area	22.0	52.0	64.0
- Reader Area	54.0	92.0	113.0

From overall reliability properties, HOC 16 Å is the optimum condition for head media spacing reduction. Thin adhesion layer and a good bonding between DLC and magnetic layer is a key for a good reliability.

5.2 Suggestions for further work

In this study, effect of HOC thickness on HGA reliability was investigated. However, to optimize HOC for HMS reduction, further studies should be focus on

-Material of adhesion layer

-Bonding between adhesion layer and DLC layer

-Optimum thickness of each adhesion layer

-Optimum thickness of each DLC layer

-Coating process for standard deviation reduction

REFERENCES

[1] Marchon B., Pitchford T., Hsia Y. T. and Gangopadhyay S. "The Head-Disk Interface Roadmap to an Area Density of 4 Tbit/in^2" **Advances in Tribology**, vol. 2013, 2013, pp. 1-8

[2] Yasui N., Inaba H., Furusawa K., Saito M. and Ohtake N. "Characterization of Head Overcoat for 1 Tb/in^2 Magnetic Recording", **IEEE Transaction on Magnetics**, vol. 45, 2009, pp. 805-809, 2009

[3] Phetdee K., Pimpim A. and Srituravanich W. "Investigation of Wear Resistance and Lifetime of Diamond-like Carbon (DLC) Coated Glass Disk in Flying Height Measurement Process" **Microsystem Technology**, vol.17, 2011, pp.1373-1379

[4] Fang C., Joel W. H. and Yongping G. **"Adhesion Layer For Protective Overcoat"** U.S. Patent no.7495865 B2, February 2009

[5] Jeong-Seok K., Dong-Ho O., Tae-yeon H. **"Head Gimbal Assembly of Hard Disk Drive"** U.S. Patent no.7050267 B2, May 2006

[6] Andrea F. C. "Diamond-like Carbon for Magnetic Storage Disks" **Surface and Coating Technology**, vol. 180-181, 2004, pp. 190-206

[7] Srinivasan G.K., Paul F.D., Cheung C.O., Allan R.F. and Paul S.W. **"Carbon Overcoat with Electrically Conductive Adhesive Layer for Magnetic Head/Slider"** U.S. Patent no.5654805, August 1997

[8] Prommanusorn School. **"Electrochemistry"** [Online]. Available: http://www.promma.ac.th/main/chemistry/web_electrochemistry/new_page_26.html 2015.

[9] Ki-Tag J., Yong-Chul Y. and Yoon-Qyu K. **"Head Gimbal Assembly of Hard Disk Drive"** U.S. Patent no.0130175 A1, June 2008

[10] Yasuyuki G., Norikazu N., Akiyo M., Hiroshi C. and Keiji W., "Head Disk Interference Technologies for High Recording Density and Reliability", **Fujitsu Science and Technology Journal** vol. 42, 2006, pp.113-121, 2006

[11] Horng C. T. and Change J.-W.. **"Bilayer Carbon Overcoating for Magnetic Data Storage Disks and Magnetic Head/Slider construction"** U.S. Patent no. 6524687 B2, February 2003

[12] Brusic V., Russak M., Schad R., Frankel G., Selius A., Dimilia D. and Edmonson D. "Corrosion of Thin Film Magnetic Disk : Galvanic Effects of the Carbon Overcoat", **Journal of the Electrochemical Society**, vol. 136, pp. 42-46, 1989

[13] Ishihara Y., Maeda F. and Kawahara H. **"Overcoat Magnetic Head Slider Having Overcoat and Magnetic Disk Device"** U.S. Patent no. 5805380 A, September 1998

[14] Kobsiriphat W., Supadee L. and Siangchaew K. "Electrochemical Impedance Characterization of Ultra-thin Carbon Overcoat" **ECS Transactions**, vol. 29, pp. 151-167, 2010

[15] Kobayashi R., Isozaki M. and Kusakawa K. "HDI Technology for Perpendicular Magnetic Recording" **Fuji Electric Review**, vol. 57, pp. 51-56, 2011

[16] Seagate Technology (Thailand) Ltd. **"Basic Electrical Parameters".** [Slide]. Samutprakarn. 2006.

[17] TDK Global. "**Magnetic Application Product**" [Online]. Available: http://www.global.tdk.com/ir/ir_library/annual/2011/html/segment/seg02.html 2015

[18] Radio Electronic "**Bit Error Rate Testing**" [Online]. Available: http://www.radio-electronics.com/info/rf-technology-design/ber/bit-error-rate-testing-bert.php 2015

[19] Suranaree University of Technology **"Metal"** [Online]. Available: http://www.sut.ac.th/engineering/Metal/pdf/Chem%20Met%20Lab/3_53/Lab_8_Galvanic_corrosion.pdf 2015

[20] ESPEC **"Test Handbook"** [Online]. Available: http://www.testnavi.com/eng/research/handbook/pdf/07_TheConceptOfRelativeHumidityInHAST.pdf 2015

APPENDIX A

PUBLICATION

(1) S. Khamdee and W. Wongwiriyapan

“Study on Head Overcoat Thickness Of Head Gimbal Assembly For Head Media Spacing Reduction” Proceedings of the 2th International Academic Conference on Engineering and Innovations”, Kuala Lumpur, Malaysia, July 16, 2015

Paper ID: AW-IACETIBANGK-12075-214

The Res

academics world

INSTITUTE OF RESEARCH ENGINEERS AND SCIENTISTS

International Academic Conference on Engineering, Technology and Innovations

Certificate

This is to certify that Sarinya Khamdee has presented a paper entitled “Study On Head Overcoatthickness Of Head Gimbal Assemblyfor Head Media Spacing Reduction” at the International Academic Conference on Engineering, Technology and Innovations (IACETI) held in Kuala Lumpur, Malaysia on 16th July 2015.

Chairman
The Institute of Research Engineers and Scientists

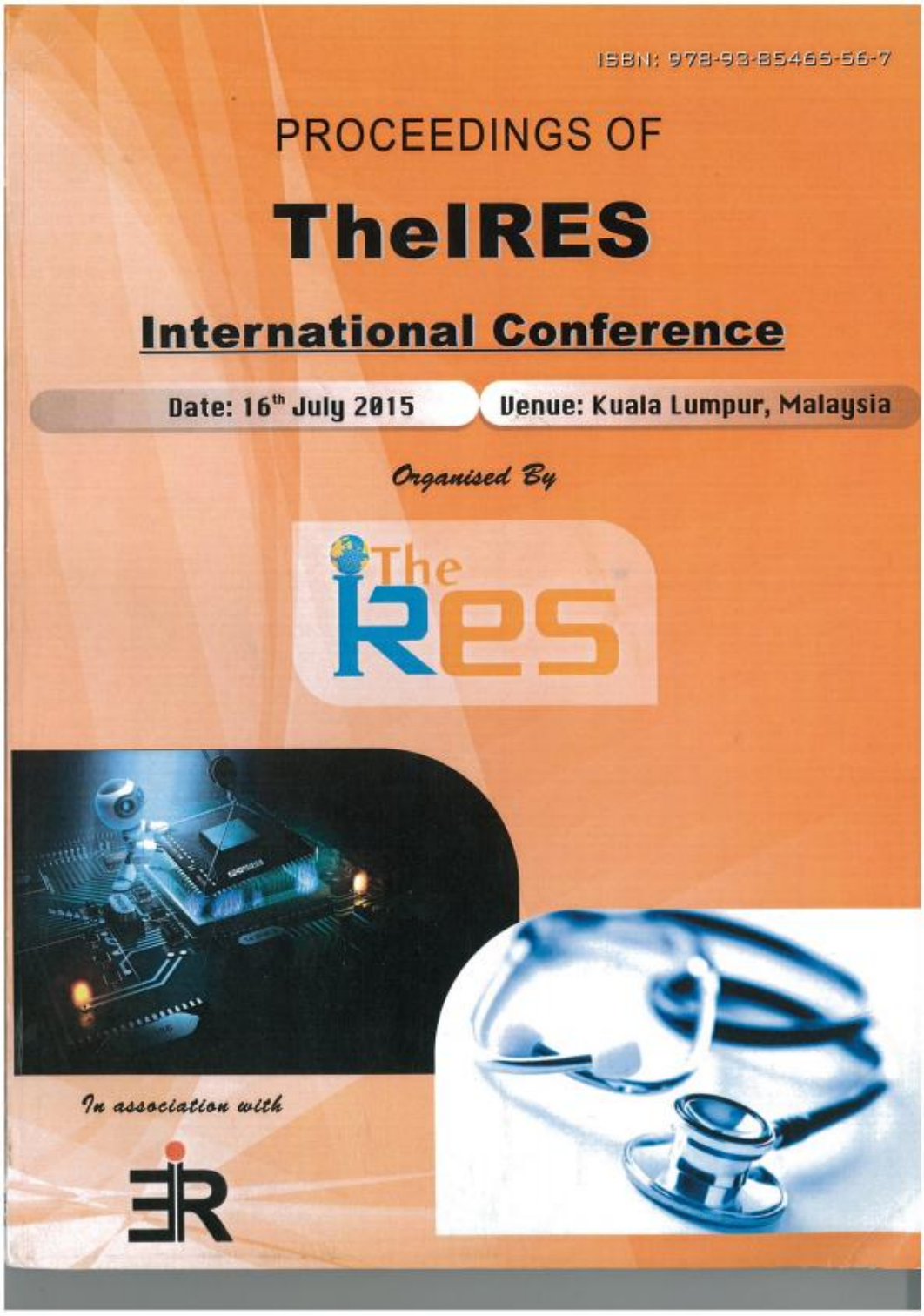
ISBN: 978-93-85465-56-7
PROCEEDINGS OF
TheIRES
International Conference
Date: 16th July 2015
Venue: Kuala Lumpur, Malaysia
Organised By
The IRES
In association with

STUDY ON HEAD OVERCOAT THICKNESS OF HEAD GIMBAL ASSEMBLY FOR HEAD MEDIA SPACING REDUCTION

[1]SARINYA KHAMDEE, [2]WINADDA WONGWIRIYAPAN
[1]College of Data Storage Innovation, King Mongkut's Institute of Technology Ladkrabang, Thailand
[2]College of Nanotechnology, King Mongkut's Institute of Technology Ladkrabang, Thailand
Email: [1]sarinya.khamdee@seagate.com, [2]kwwinadd@kmitl.ac.th

Abstract: Effect of head overcoat (HOC) thickness of head gimbal assembly (HGA) for head media spacing (HMS) reduction was investigated. HOCs with thickness of 16, 20 and 24 Å were used in this study. Reliability, read/write performance and active fly height were evaluated on spin-stand tester by electrical measurement at designated HGA level and wear were characterized by field-emission electron microscope. From electrical measurements that burnishing head from +1 nm to -4 nm, HOC 16 Å shows the best reliability as degradation of read/write performance is least degradation rate, implying no significant effect to read/write performance. Furthermore, HOC 16 Å has only light wear on transducers. From above results, HOC 16 Å is a promising thickness for HMS reduction with maintaining good reliability.

Keywords: Head Overcoat, Head Media Spacing, Head Gimbal Assembly, Electrical Degradation, FESEM

1. INTRODUCTION

Currently, due to a need to increase areal density of hard disk drive (HDD), many technologies have been developed. The main development is focused on transducer design. However, transducer design for perpendicular magnetic recording (PMR) is nearly to reach its limitation, while technology will be switched to heat assist magnetic recording (HAMR) in the near future. Prior to changing to HAMR technology, the critical approach to reach higher areal density for PMR technology is head media spacing (HMS) reduction. HMS is head overcoat including touch down height, clearance, media lubricant and media overcoat [1]. There are many technologies have been developed to reduce HMS such as air bearing design, thermo mechanical design, media overcoat and head overcoat (HOC) [2].

Currently, HMS is ca. 12-15 nm and fly height is ca. 10 nm. To increase areal density, it is estimated that the HMS should be lower than 10 nm. A decrease in HOC thickness is one factor for HMS reduction. However, extremely thinner HOC might lead to poor long-term reliability. Thus, it is necessary to investigate the optimum HOC thickness with good reliability.

HOC is diamond-like carbon (DLC) layer including adhesion layer. The function of adhesion layer [3] is to provide a good bonding surface for DLC layer which deposited on the top. The function of DLC layer [4] is to protect head from wear and corrosion. Typical thickness range of HOC is ca. 20-30 Å, which DLC layer thickness is ca. 15-25 Å and adhesion layer thickness is ca. 5-8 Å. A schematic view of HOC layer is shown in **Fig.1**

In this study, taking a decrease in HOC thickness as a strategy for HMS reduction, the effect of HOC thickness on HDD performance was investigated.

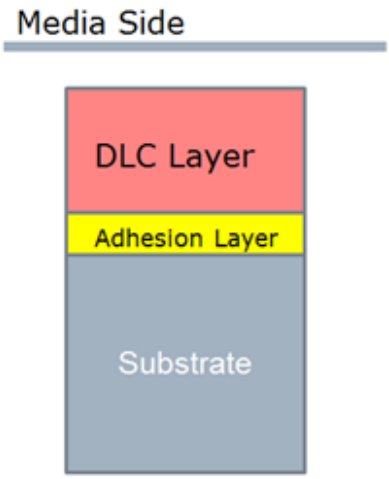

Fig.1. A schematic view of HOC layer which consists of DLC and adhesion layers

2. DETAILS EXPERIMENTAL

HOCs with 3 various thicknesses; 16Å, 20Å and 24Å, have been evaluated. To investigate read/write ability of each HOC thickness, electrical measurement was done on spin-stand tester for reliability test with stressed burnishing.

The test algorithm is dwelling the head interference by stepping clearance level from +1 nm to -4 nm with a step size of 0.5 nm to monitor degradation of electrical performance at each interference level. Flow of test algorithm is shown in **Fig.2**.

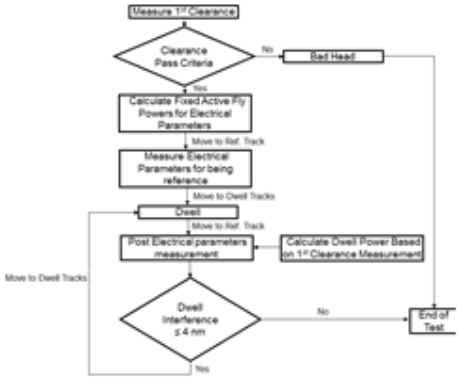

Fig.2. Test algorithm

Besides investigation read/write ability of head by electrical performance, field-emission electron microscopy (FESEM) was utilized to investigate wear and contamination that may occur during read/write process. FESEM images were taken on air bearing surface and FESEM image of writer pole was recorded at high magnification.

3. RESULTS AND DISCUSSION

3.1. Electrical Measurement

Before burnishing and measuring read/write performance, it needs to conduct electrical measurement to measure power to contact and clearance to use as a reference value. The result is shown in **Table 1**.

Table 1: Results of Electrical Measurement before Burnishing

Parameters	HOC Thickness (Å)		
	24	20	16
Power to Contact (mW)	79.74±5.00	82.52±5.80	85.14±3.96
Clearance (nm)	10.42±0.66	10.51±0.78	10.69±0.54
Bit Error Rate (dcd)	-2.23±0.24	-2.25±0.28	-2.13±0.17
Overwrite (dB)	-39.29±3.35	-36.35±3.23	-35.08±1.46
Amplitude (μV)	13,415±3,509	16,185±4,801	13,727±3,711
Reader Resistance (Ω)	214.92±2685	248.18±3996	266.28±39.16

Data of power to contact and clearance of each thickness is reasonable and follows the trend which HOC 16 Å shows the highest value where HOC 24 Å is lowest. When head has been loaded to over the media on same machine, head stays at the same point.

After electrical measurement, head was moved to dwell at the designated interference level and the head was burnished. Then the head was moved back to reference track for electrical measurement again. The data of electrical measurement after burnishing will be compared with reference data for calculating degradation of each electrical parameter. This result is shown in **Fig.3**.

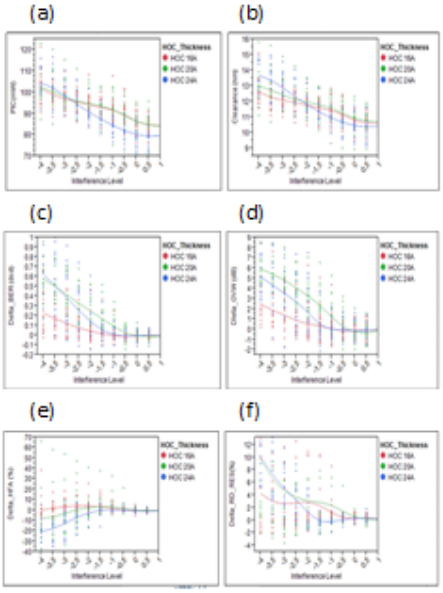

Fig.3. Degradation result of key electrical parameters at any interference level. (a) Contact power, (b) Clearance, (c) Delta bit error rate, (d) Delta overwrite, (e) Delta amplitude and (f) Delta reader resistance.

Power to contact (PtC) and clearance as shown in **Figs. 3(a) and 3(b)** have the same trends for each HOC thickness. When increase interference level, power to contact and clearance increase and a change rate is relatively linear.

Read/write ability can be described by degradation rate of bit error rate (BER), overwrite (OVW), amplitude (HFA) and reader resistance (RD_RES) (**Figs.3(c)-3(f)**). When HOC thickness increases, degradation increases. HOC 16 Å shows just slightly degradation when increase interference level to maximum interference level (-4 nm) for all key electrical parameters such as only 4% degradation of reader resistance. HOCs 20 Å and 24 Å show high degradation when increase interference level to maximum interference level (-4 nm). HOC 20Å is slightly less degradation rate than HOC 24 Å.

3.2. FESEM Result

After electrical measurement, head was characterized by FESEM to investigate wear and contamination [5]. **Fig.4**. shows FESEM image of each HOC thickness.

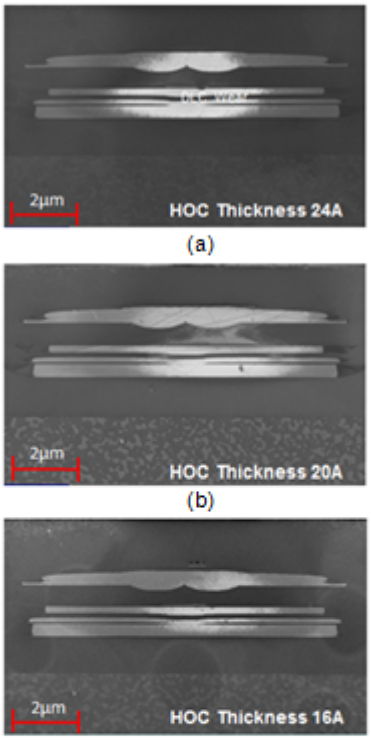

Fig.4. FESEM images HOC with thickness of (a) 24 Å, (b) 20 Å and 16 Å

Wear was appeared at pole tip for all samples. Electrical measurement simulates as head flying into the media layer so it is reasonable to see wear on pole tip, implying that head really contacted the media. FESEM images show that HOC 16 Å and 20 Å have light wear while HOC 24 Å has heavy wear at pole tip. This result can be explained by electrical parameters.

This phenomenon is directly related with HOC thickness. In the ideal case, thicker thickness should have the least wear, however, in actual, bonding between DLC and adhesion layers of each HOC thickness might be different. Read/write process might lead to make thickness thinner as poor bonding then easily to lost bonding while head flying.

CONCLUSIONS

Effect of HOC thickness on the effect of on HDD performance was investigated. The lowest HOC thickness (HOC 16 Å) shows the best reliability than thicker thickness (HOCs 20 Å and 24 Å) with low degradation rate, more robustness and light wear. However, lowering HOC thickness and bonding between DLC layer and adhesion layer still need to be further studied to obtain optimum thickness for HMS reduction.

ACKNOWLEDGMENTS

The authors would like to acknowledge the College of Data Storage Innovation, King Mongkut's Institute of Technology Ladkrabang and Seagate Technology (Thailand) Co., Ltd. for all equipment and material supporting.

REFERENCES

1. M. Bruno, P. Thomas, H. Yiao-Tee and G. Sunita "The Head-Disk Interface Roadmap to an Area Density of 4 Tbit/in2", Hindawi Publishing Corporation Advance in Tribology, vol 2013,article ID 521086,8 pages, 2013.
2. C. Fang, H. W. Joel, and G. Yongping, "Adhesion Layer For Protective Overcoat", United States Patent, Patent No.7495865 B2,2009
3. G. Yasuyuki, N. Norikazu, M. Akiyo, C. Hiroshi and W. Keiji, "Head Disk Interference Technologies for High Recording Density and Reliability", Fujitsu Sci.Tech.J,vol.42,pp.113-121,2006.
4. P. Korakoch, P. Alongkorn and S. Werayut, "Investigation of wear resistance and lifetime of diamond-like carbon (DLC) coated glass disk in flying height measurement process" Microsyst Technol, vol.17, pp.1373-1379,2011
5. F. C. Andrea "Diamond-like carbon for magnetic storage disks" Surface and Coating Technology, vol. 180-181.pp 190-206,2004

★★★

AUTHOR BIOGRAPHY

Name-Surname: Ms. Sarinya Khamdee

Date of Birth: November 7th, 1983

Present Address: 1033/20, Srinakarindra Rd., Suanluang District, Bangkok, Thailand 10250

Education: 2003-2006: Bachelor degree in Electrical engineering, Srinakariinwirot University, Thailand

Scholarships: 2010-2011 Scholarship for study in Master of Engineering in Data Storage Technology (English program) by NSTDA, KMITL and Seagate Technology (Thailand) Ltd.

Publications: S. Khamdee. "STUDY ON HEAD OVERCOAT THICKNESS OF HEAD GIMBAL ASSEMBLY FOR HEAD MEDIA SPACING REDUCTION", IACETI 2015, 2th International Data Storage Technology Conference at Kuala Lumpur, Malaysia, July 16, 2015

Experience: 2008-Present Seagate Technology (Thailand) Ltd.

- 2008 to 2010 Test Engineer (New product support)
- 2010 to 2012 Product Test Engineer
- 2012 to present Mechanical Design Verification Test Engineer